A MICROMECHANICS MODEL OF THERMAL EXPANSION COEFFICIENT IN FIBER REINFORCED COMPOSITES

by

NITTAPON SRISUK

Presented to the Faculty of the Graduate School of
The University of Texas at Arlington in Partial Fulfillment
of the Requirements
for the Degree of

MASTER OF SCIENCE IN AEROSPACE ENGINEERING

THE UNIVERSITY OF TEXAS AT ARLINGTON

December 2010

ACKNOWLEDGEMENTS

I would like to acknowledge my supervising professor Dr. Wen S. Chan for his invaluable guidance and encouragement and support that helped me throughout the entire academic program. Without his patient and attentive guidance, this thesis would not been possible.

Also, I would like to thank Dr. Erian Armanios and Dr. Seiichi Nomura, the members of committee, for their comments and for taking time to serve in my thesis committee.

I would also like to extend my appreciation to Royal Thai Air Force, especially Directorate of Aeronautical Engineering, for providing scholarship for my study.

I also wish to thank the former students of Dr. Chan's, Mr. Selvaraj and Dr. Rios, for their assistance in developing ANSYS code. In addition, I would also like to thank all of my friends for their support and encouragement.

Finally, I specially thank my parents and family for their support and encouragement during this study period.

November 1, 2010

ABSTRACT

A MICROMECHANICS MODEL OF THERMAL EXPANSION COEFFICIENT IN FIBER REINFORCED COMPOSITES

NITTAPON SRISUK, M.S.

The University of Texas at Arlington, 2010

Supervising Professor: Wen Chan

Fiber reinforced composites are widely used for the various applications in the aerospace, automotive, infrastructures and sporting goods industries. The evaluations of its mechanical and thermal properties are needed for accurate estimation of their structural response.

In this study, a mathematical closed-form expression of unit cell model was developed to estimate the coefficient of thermal expansion (CTE) along longitudinal and transverse directions of unidirectional lamina. Unlike the previous models, the present model takes into consideration of the fiber configuration and volume fraction of each constituent in the unit cell. In addition, the model is also able to obtain the stresses of the fiber and matrix of unit cell under the temperature environment. The results obtained by present model was validated by ANSY finite model.

The parametric study was conducted to better understanding the effect of the CTEs on the fiber volume fraction and fiber configuration. Comparison of the CTEs results obtained by the rule-of-mixture (ROM) and Shaperys model as well as the FEM was conducted. The results of longitudinal CTE are in excellent agreement

among all of the models. In the transverse CTE, the present result has better agreement with the FEM result than with the other models. The present results also indicate that changing the fiber configurations does affect the transverse CTE but not longitudinal CTE.

TABLE OF CONTENTS

LIST OF FIGURES

CHAPTER 1

INTRODUCTION

1.1 Background

Structural applications of composite materials require accurate estimation of structural response in different temperature environments. The coefficient of thermal expansion (CTE) is the thermoelastic property that shows the response of the material geometry when the temperature is changed. In composite materials, the CTE is more complex than that in isotropic materials. There are three well-known methods to evaluate the properties of fiber reinforced composite, especially the CTEs.

First of all, the CTEs and the other properties of fiber reinforced composite can be experimentally characterized in the laboratory. The specimens of the materials will be tested under the uniform thermal load in steady state condition. Among there, the transverse and longitudinal CTEs were measured in the experiment of Kulkarni and Ochoa[1]. Kia[2] also measured the CTEs from the experiments in sheet molding compound (SMC) composites. However, the experiment will be considerably costly and time consuming when appraising in the materials with some parameters studies such as the fiber volume fraction and configuration. In addition, the most experiments were focused on the effects of temperature not the volume fraction and configuration of fiber.

Secondly, many analytical models were created for evaluating the composite properties, includes the CTEs, in different material systems. Among them, the rule-of-mixture (ROM) model which was based upon the linear or reciprocal linear relationship of the fiber and matrix fraction to determine the properties. Schapery[3]

used energy principles to determine the longitudinal and transverse CTEs of unidirectional composites. Likewise, Rosen and Hashin[4] also derived the CTEs estimation based on thermoelastic energy principles. The transverse CTE is more complex for prediction. Therefore, some researches only focused in the evaluation of transverse CTE such as Tandon and Chatterjee[5]. Ishikawa, Koyama and Kobayashi[6] derived the analytical solution and conducted the experiment to evaluate the CTEs in both directions. Moreover, Melo and Radford[7] determined the properties, includes the CTEs analytically and experimentally for the different angle ply of the composite laminates. Wang and Chan[8] developed an analytical model of unit cell to evaluated the stiffness of composite rod reinforced lamina. Both circular and elliptical cross-sections of composite rods were studied. Likewise, the micromechanics model of square array unit cell of heterogeneous materials were formed for predicting the CTEs by Yu and Tang[9].

With the development in computer technology, the numerical solutions, especially the finite element analysis (FEA), are also employed to study the CTEs. 2D-FEM models of the square array of fiber reinforced composite with and without cracked were created in ABAQUS program to solve both longitudinal and transverse CTEs by Islam, Sjolind and Pramila[10]. Kulkarni and Ochoa[1] also used 2D-FEM model of the representative volume element (RVE) of the hexagonal array of fiber reinforced composites to solve the CTEs in both directions. Moreover, 3D FEM model of ANSYS was used to study the CTEs for fiberous reinforced composites and the results were used to compare with analytical solutions by Karadeniz and Kumlutas[11].

1.2 Objective of Research

The objective of this thesis is to modify the unit cell model of Wang and Chan[8] to evaluate the CTEs of the uni-directional composite lamina in both longitudinal and

transverse directions. With this in mind, the new micromechanics model is developed by adding the terms of thermal strain in order to estimate the CTEs in the analytical solution. Furthermore, the stresses in fiber and matrix are also obtained from the developed micro-mechanics model. Also, the FEM model is developed to calculate the CTEs. Moreover, the models of both analytical and finite element models are used to study the effect of CTE's due to the fiber configuration and the fiber volume fraction in the unit cell.

1.3 Outline of This Thesis

In Chapter 2, a micromechanics model of the unit cell composite laminates is developed to evaluate the laminated stiffness matrix and the thermal resultant force and moment matrix. With these properties, the effective moduli and CTEs can be also obtained.

In Chapter 3, the finite element models are developed to obtain the deformation and strain in each model for calculating the effective moduli and CTEs of the unit cell fiber reinforced laminates. The result of the FEM model is also used for validation of the composite properties calculated by an analytical solution.

The parameter study on the fiber volume fraction and the fiber configuration for CTE's is conducted and their results were studied in Chapter 4.

Conclusion and future work are presented in Chapter 5.

CHAPTER 2

ANALYTICAL MODEL WITH THERMAL EXPANSION

The unit cell is chosen for a representative from the whole microstructure as shown in Figure 2.1. The unit cell fiber reinforced layer is featured two portions that are fiber and matrix. The fiber that is stiffer than the matrix material is positioned at the center of the unit cell layer. The fiber can be both orthotropic and isotropic materials. Unlikely, the matrix is generally the isotropic material. The model developed by Wang and Chan[8] was for evaluating the stiffness matrix of unidirectional lamina. No the coefficient of thermal expansion (CTE) and stresses components of the fiber and matrix were obtained. The objective of this chapter is to modify the previous analytical method by including the thermal term in the model. With this condition, the CTE's of the unit cell fiber reinforced laminated will be obtained. The model presented in this chapter will be able to obtain the lamina CTE's and the stress components of the fiber and matrix due to temperature. The variations of the laminate stiffness matrix, effective moduli and the CTE's respect with the fiber volume fraction are also studied. Secondly, the cross section of the fibers may vary from elliptical to circular configuration with the given fiber volume. Therefore, evaluation of laminate stiffness matrix, effective moduli and CTE variations due to various configuration of axial ratio is also investigated.

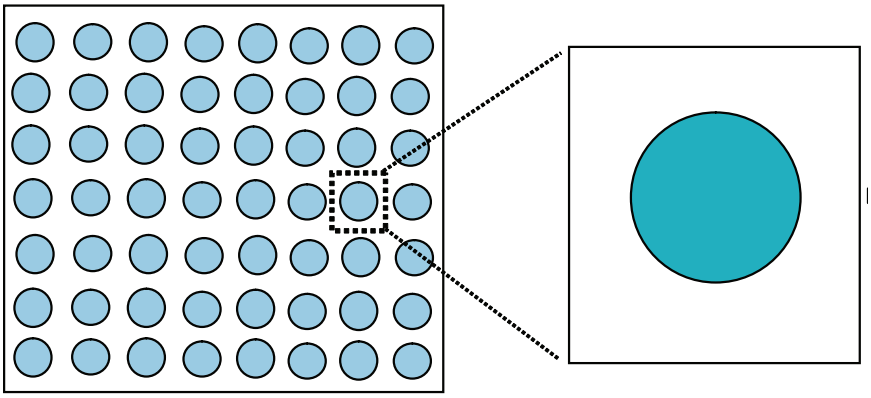

Figure 2.1. Microstructure and Unit Cell of Fiber Reinforced Composite.

2.1 Approach of Analytical Model Development

The unit cell layer contains an elliptical fiber that is surrounded by the matrix. The cross-sectional area of the unit cell layer is shown in Figure 2.2. The elliptical cross-section of fiber configuration is used in this model due to the interesting in fiber configuration effect. The fiber and matrix are assumed to be orthotropic and isotropic, respectively. The semi major and minor axis of the elliptical fiber are designated in the symbol a and b, respectively. Likewise, the width and thickness (or also height) of the unit cell layer are represented in W and h.

In the past work, a unit cell was divided into two regions, fiber and matrix, respectively according to their fiber volume fraction. In doing so, the configuration of fiber in the unit cell is ignored. In this approach, the cross section of the unit cell layer is divided into sub-layers in z direction as shown in Figure2.3.

In the following derivation, σ, τ, ε, γ and α are the normal stress, shear stress, normal strain, shear strain, and coefficient of thermal expansion, respectively. In addition, the subscripts f and m, refer to the fiber and matrix constituents and the subscripts 1 and 2, refer to the layer properties along the fiber and transverse to fiber

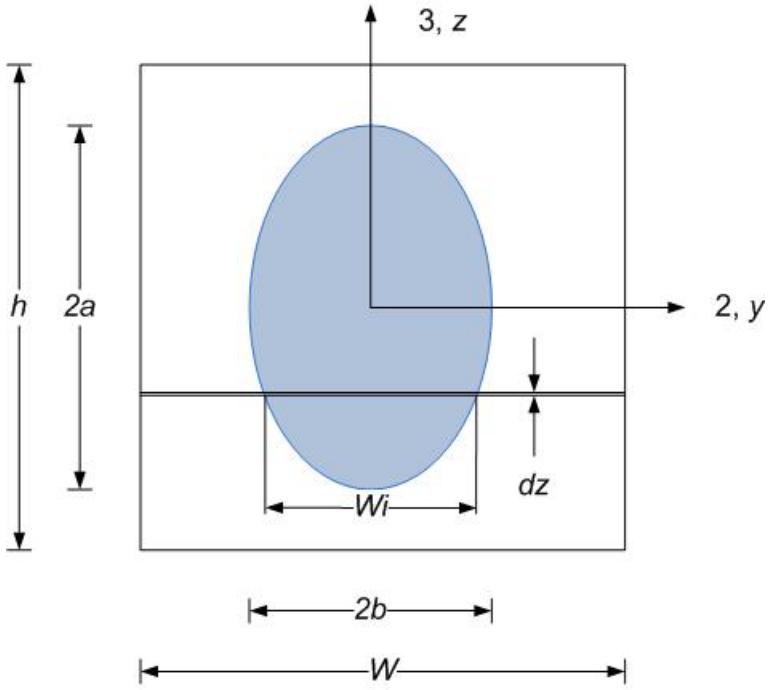

Figure 2.2. Cross-Sectional Area and Geometry of Unit Cell.

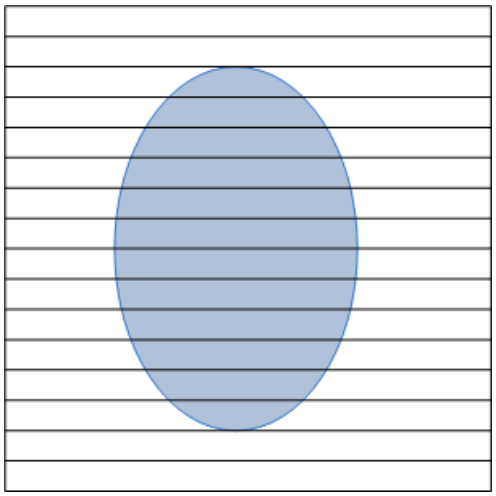

Figure 2.3. Example of Sub-layer in Unit Cell.

directions, respectively. Finally, the superscript, T refers to the total strain which includes the mechanical and the thermal strain components. Perfect bonding between

fiber and its surrounding matrix and no void in the fiber-layer are assumed. With these assumptions, the following relations can be established:

$$\varepsilon_1^T = \varepsilon_{1f}^T = \varepsilon_{1m}^T \tag{2.1}$$

$$\sigma_2 = \sigma_{2f} = \sigma_{2m} \tag{2.2}$$

$$\tau_{12} = \tau_{12f} = \tau_{12m} \tag{2.3}$$

$$\sigma_1 = \sigma_{1f} V_f + \sigma_{1m} V_m \tag{2.4}$$

$$\varepsilon_2^T = \varepsilon_{2f}^T V_f + \varepsilon_{2m}^T V_m \tag{2.5}$$

$$\gamma_{12} = \gamma_{12f} V_f + \gamma_{12m} V_m \tag{2.6}$$

$$V_f + V_m = 1 \tag{2.7}$$

Where V_f and V_m are the volume fractions of the fiber and the matrix in the layer, respectively.

The fiber volume fraction, V_f in each sub-layer can be written from the geometry of the fiber as

$$V_f = \begin{cases} 0 & z \in [\frac{-h}{2}, -a] \cup [a, \frac{h}{2}] \\ \frac{w_i}{W} = \frac{2b}{W}\sqrt{1 - \frac{z^2}{a^2}} & z \in [-a, a] \end{cases} \tag{2.8}$$

Where w_i is the width of the fiber part of each sub-layer.

2.2 Reduced Stiffness Matrix of Sub-layer

The constitutive equation of each constituent in the sub-layer is written as the below equations.

For the fiber constituent,

$$\begin{bmatrix} \sigma_{1f} \\ \sigma_{2f} \\ \tau_{12f} \end{bmatrix} = \begin{bmatrix} Q_{11f} & Q_{12f} & 0 \\ Q_{12f} & Q_{22f} & 0 \\ 0 & 0 & Q_{66f} \end{bmatrix} \begin{bmatrix} \varepsilon_{1f} \\ \varepsilon_{2f} \\ \gamma_{12f} \end{bmatrix}$$

Substituting (2.1) into the above equation, we have

$$\begin{bmatrix} \sigma_{1f} \\ \sigma_{2f} \\ \tau_{12f} \end{bmatrix} = \begin{bmatrix} Q_{11f} & Q_{12f} & 0 \\ Q_{12f} & Q_{22f} & 0 \\ 0 & 0 & Q_{66f} \end{bmatrix} \begin{bmatrix} \varepsilon_1^T - \alpha_{1f}\Delta T \\ \varepsilon_{2f}^T - \alpha_{2f}\Delta T \\ \gamma_{12f} \end{bmatrix} \tag{2.9}$$

For the matrix constituent,

$$\begin{bmatrix} \sigma_{1m} \\ \sigma_{2m} \\ \tau_{12m} \end{bmatrix} = \begin{bmatrix} Q_{11m} & Q_{12m} & 0 \\ Q_{12m} & Q_{22m} & 0 \\ 0 & 0 & Q_{66m} \end{bmatrix} \begin{bmatrix} \varepsilon_{1m} \\ \varepsilon_{2m} \\ \gamma_{12m} \end{bmatrix}$$

$$\begin{bmatrix} \sigma_{1m} \\ \sigma_{2m} \\ \tau_{12m} \end{bmatrix} = \begin{bmatrix} Q_{11m} & Q_{12m} & 0 \\ Q_{12m} & Q_{22m} & 0 \\ 0 & 0 & Q_{66m} \end{bmatrix} \begin{bmatrix} \varepsilon_1^T - \alpha_{1m}\Delta T \\ \varepsilon_{2m}^T - \alpha_{2m}\Delta T \\ \gamma_{12m} \end{bmatrix}$$

The matrix is the isotropic material. Therefore, $\alpha_{1m} = \alpha_{2m} = \alpha_m$

$$\begin{bmatrix} \sigma_{1m} \\ \sigma_{2m} \\ \tau_{12m} \end{bmatrix} = \begin{bmatrix} Q_{11m} & Q_{12m} & 0 \\ Q_{12m} & Q_{22m} & 0 \\ 0 & 0 & Q_{66m} \end{bmatrix} \begin{bmatrix} \varepsilon_1^T - \alpha_m \Delta T \\ \varepsilon_{2m}^T - \alpha_m \Delta T \\ \gamma_{12m} \end{bmatrix} \tag{2.10}$$

For the whole unit cell layer,

$$\begin{bmatrix} \sigma_1 \\ \sigma_2 \\ \tau_{12} \end{bmatrix} = \begin{bmatrix} Q_{11} & Q_{12} & 0 \\ Q_{12} & Q_{22} & 0 \\ 0 & 0 & Q_{66} \end{bmatrix} \begin{bmatrix} \varepsilon_1 \\ \varepsilon_2 \\ \gamma_{12} \end{bmatrix}$$

$$\begin{bmatrix} \sigma_1 \\ \sigma_2 \\ \tau_{12} \end{bmatrix} = \begin{bmatrix} Q_{11} & Q_{12} & 0 \\ Q_{12} & Q_{22} & 0 \\ 0 & 0 & Q_{66} \end{bmatrix} \begin{bmatrix} \varepsilon_1^T - \alpha_1 \Delta T \\ \varepsilon_2^T - \alpha_2 \Delta T \\ \gamma_{12} \end{bmatrix} \tag{2.11}$$

Substituting both Equations (2.9) and (2.10) into Equations (2.2), (2.3) and (2.4), we obtain

$$\begin{aligned} \sigma_1 = {} & (Q_{11f} V_f + Q_{11m} V_m) \varepsilon_1^T + Q_{12f} V_f \varepsilon_{2f}^T + Q_{12m} V_m \varepsilon_{2m}^T \\ & - [(Q_{11f} \alpha_{1f} + Q_{12f} \alpha_{2f}) V_f + (Q_{11m} \alpha_m + Q_{12m} \alpha_m) V_m] \Delta T \end{aligned} \tag{2.12}$$

With $\sigma_2 = \sigma_{2f}$, we have

$$\sigma_2 = Q_{12f} \varepsilon_1^T + Q_{22f} \varepsilon_{2f}^T - (Q_{12f} \alpha_{1f} + Q_{22f} \alpha_{2f}) \Delta T \tag{2.13}$$

Since $\sigma_2 = \sigma_{2m}$, we have

$$\sigma_2 = Q_{12m} \varepsilon_1^T + Q_{22m} \varepsilon_{2m}^T - (Q_{12m} \alpha_m + Q_{22m} \alpha_m) \Delta T \tag{2.14}$$

$$\tau_{12f} = Q_{66f}\gamma_{12f} \tag{2.15}$$

$$\tau_{12m} = Q_{66m}\gamma_{12m} \tag{2.16}$$

Where ε_{2f}^T and ε_{2m}^T are still unknown and they will be expressed in the term of ε_1^T, ε_2^T and ΔT.

From the constitutive equation of each constituent in the sub-layer, the following relationships can be obtained.

$$\sigma_{2f} = Q_{12f}\varepsilon_1^T + Q_{22f}\varepsilon_{2f}^T - (Q_{12f}\alpha_{1f} + Q_{22f}\alpha_{2f})\Delta T \tag{2.17}$$

$$\sigma_{2m} = Q_{12m}\varepsilon_1^T + Q_{22m}\varepsilon_{2m}^T - (Q_{12m}\alpha_m + Q_{22m}\alpha_m)\Delta T \tag{2.18}$$

Since $\sigma_{2f} = \sigma_{2m}$, we can rewrite ε_{2f}^T and ε_{2m}^T as shown below

$$\varepsilon_{2m}^T = \frac{1}{Q_{22m}}[(Q_{12f} - Q_{12m})\varepsilon_1^T + Q_{22f}\varepsilon_{2f}^T + (Q_{12m}\alpha_m + Q_{22m}\alpha_m - Q_{12f}\alpha_{1f} - Q_{22f}\alpha_{2f})\Delta T] \tag{2.19}$$

$$\varepsilon_{2f}^T = \frac{1}{Q_{22f}}[(Q_{12m} - Q_{12f})\varepsilon_1^T + Q_{22m}\varepsilon_{2m}^T + (Q_{12f}\alpha_{1f} + Q_{22f}\alpha_{2f} - Q_{12m}\alpha_m - Q_{22m}\alpha_m)\Delta T] \tag{2.20}$$

Substituting Equations (2.19) and (2.20) into Equation (2.5) respectively, then ε_{2f}^T and ε_{2m}^T can be obtain in terms of ε_1^T, ε_2^T and ΔT as expressed:

ε_{2f}^T is firstly considered.

$$\varepsilon_2^T = \varepsilon_{2f}^T V_f + \frac{V_m}{Q_{22m}}[(Q_{12f} - Q_{12m})\varepsilon_1^T + Q_{22f}\varepsilon_{2f}^T + (Q_{12m}\alpha_m + Q_{22m}\alpha_m - Q_{12f}\alpha_{1f} - Q_{22f}\alpha_{2f})\Delta T]$$

$$\begin{aligned}\varepsilon_2^T = {} & \frac{Q_{22m}V_f + Q_{22f}V_m}{Q_{22m}}\varepsilon_{2f}^T + \frac{V_m(Q_{12f} - Q_{12m})}{Q_{22m}}\varepsilon_1^T \\ & + \frac{V_m}{Q_{22m}}(Q_{12m}\alpha_m + Q_{22m}\alpha_m - Q_{12f}\alpha_{1f} - Q_{22f}\alpha_{2f})\Delta T\end{aligned}$$

$$\begin{aligned}\varepsilon_{2f}^T = {} & \frac{Q_{22m}}{Q_{22m}V_f + Q_{22f}V_m}\varepsilon_2^T + \frac{V_m(Q_{12m} - Q_{12f})}{Q_{22m}V_f + Q_{22f}V_m}\varepsilon_1^T \\ & + \frac{V_m(Q_{12f}\alpha_{1f} + Q_{22f}\alpha_{2f} - Q_{12m}\alpha_m - Q_{22m}\alpha_m)}{Q_{22m}V_f + Q_{22f}V_m}\Delta T\end{aligned} \tag{2.21}$$

Similarly, ε_{2m}^T can be obtained from Equation (2.5) as shown below.

$$\begin{aligned}\varepsilon_2^T = {} & \frac{Q_{22m}V_f + Q_{22f}V_m}{Q_{22f}}\varepsilon_{2m}^T + \frac{V_f(Q_{12m} - Q_{12f})}{Q_{22f}}\varepsilon_1^T \\ & + \frac{V_f}{Q_{22f}}(Q_{12f}\alpha_{1f} + Q_{22f}\alpha_{2f} - Q_{12m}\alpha_m - Q_{22m}\alpha_m)\Delta T\end{aligned}$$

$$\begin{aligned}\varepsilon_{2m}^T = {} & \frac{Q_{22f}}{Q_{22m}V_f + Q_{22f}V_m}\varepsilon_2^T + \frac{V_f(Q_{12f} - Q_{12m})}{Q_{22m}V_f + Q_{22f}V_m}\varepsilon_1^T \\ & + \frac{V_f(Q_{12m}\alpha_m + Q_{22m}\alpha_m - Q_{12f}\alpha_{1f} - Q_{22f}\alpha_{2f})}{Q_{22m}V_f + Q_{22f}V_m}\Delta T\end{aligned} \tag{2.22}$$

For the shear term, from Equations (2.3) and (2.15) the following relationship is obtained.

$$\gamma_{12m} = \frac{Q_{66f}\gamma_{12f}}{Q_{66m}}$$

Substituting above equation in Equation (2.6), then γ_{12f} can be obtained in terms of γ_{12}.

$$\gamma_{12} = \gamma_{12f} V_f + \gamma_{12m} V_m$$

$$\gamma_{12} = \gamma_{12f} V_f + \frac{Q_{66f}\gamma_{12f}}{Q_{66m}} V_m$$

$$\gamma_{12} = \gamma_{12f} (V_f + \frac{Q_{66f}}{Q_{66m}} V_m)$$

$$\gamma_{12f} = \frac{Q_{66m}}{Q_{66m} V_f + Q_{66f} V_m} \gamma_{12} \tag{2.23}$$

Combining Equations (2.18), (2.19) and (2.20) into Equations (2.11), (2.12) and (2.13), we can obtain the reduced stiffness of the unit cell layer in terms of the reduced stiffness of each constituent and its volume fraction. The constitutive equation of the unit cell layer can be written as Equation (2.11).

$$\begin{bmatrix} \sigma_1 \\ \sigma_2 \\ \tau_{12} \end{bmatrix} = \begin{bmatrix} Q_{11} & Q_{12} & 0 \\ Q_{12} & Q_{22} & 0 \\ 0 & 0 & Q_{66} \end{bmatrix} \begin{bmatrix} \varepsilon_1^T - \alpha_1 \Delta T \\ \varepsilon_2^T - \alpha_2 \Delta T \\ \gamma_{12}^T \end{bmatrix}$$

The reduced stiffness matrix of each sub-layer in terms of the stiffness of each constituent and its volume fraction are expressed as following.

The stress in 1-direction is considered first,

$$\sigma_1 = Q_{11}(\varepsilon_1^T - \alpha_1 \Delta T) + Q_{12}(\varepsilon_2^T - \alpha_2 \Delta T)$$

$$\sigma_1 = Q_{11}\varepsilon_1^T + Q_{12}\varepsilon_2^T - (Q_{11}\alpha_1 + Q_{12}\alpha_2)\Delta T \tag{2.24}$$

Then consider (2.12),

$$\sigma_1 = (Q_{11f}V_f + Q_{11m}V_m)\varepsilon_1^T + Q_{12f}V_f\varepsilon_{2f}^T + Q_{12m}V_m\varepsilon_{2m}^T$$
$$- [(Q_{11f}\alpha_{1f} + Q_{12f}\alpha_{2f})V_f + (Q_{11m}\alpha_m + Q_{12m}\alpha_m)V_m]\Delta T$$

Substitute ε_{2f}^T and ε_{2m}^T into Equation (2.12) and rearrange it in term of ε_1^T, ε_2^T and ΔT.

$$\begin{aligned}\sigma_1 = {} & [Q_{11f}V_f + Q_{11m}V_m + \frac{Q_{12f}V_fV_m(Q_{12m} - Q_{12f})}{Q_{22m}V_f + Q_{22f}V_m} + \frac{Q_{12m}V_mV_f(Q_{12f} - Q_{12m})}{Q_{22m}V_f + Q_{22f}V_m}]\varepsilon_1^T \\ & + [\frac{Q_{12f}Q_{22m}V_f}{Q_{22m}V_f + Q_{22f}V_m} + \frac{Q_{12m}Q_{22f}V_m}{Q_{22m}V_f + Q_{22f}V_m}]\varepsilon_2^T \\ & + [\frac{V_fV_m(Q_{12f} - Q_{12m})(Q_{12f}\alpha_{1f} + Q_{22f}\alpha_{2f} - Q_{12m}\alpha_m - Q_{22m}\alpha_m)}{Q_{22m}V_f + Q_{22f}V_m} \\ & - \{(Q_{11f}\alpha_{1f} + Q_{12f}\alpha_{2f})V_f + (Q_{11m}\alpha_m + Q_{12m}\alpha_m)V_m\}]\Delta T\end{aligned} \tag{2.25}$$

Equating (2.24) and (2.25), Q_{11} and Q_{12}can be obtained as.

$$Q_{11} = Q_{11f}V_f + Q_{11m}V_m + \frac{Q_{12f}V_fV_m(Q_{12m} - Q_{12f})}{Q_{22m}V_f + Q_{22f}V_m} + \frac{Q_{12m}V_mV_f(Q_{12f} - Q_{12m})}{Q_{22m}V_f + Q_{22f}V_m}$$

Or

$$Q_{11} = (Q_{11f} - Q_{11m})V_f + Q_{11m} - \frac{(V_f - V_f^2)(Q_{12m} - Q_{12f})^2}{(Q_{22m} - Q_{22f})V_f + Q_{22f}} \tag{2.26}$$

$$Q_{12} = \frac{Q_{12f}Q_{22m}V_f}{Q_{22m}V_f + Q_{22f}V_m} + \frac{Q_{12m}Q_{22f}V_m}{Q_{22m}V_f + Q_{22f}V_m}$$

Or

$$Q_{12} = \frac{(Q_{12f}Q_{22m} - Q_{12m}Q_{22f})V_f + Q_{12m}Q_{22f}}{(Q_{22m} - Q_{22f})V_f + Q_{22f}} \tag{2.27}$$

The thermal related terms can be obtained as

$$-(Q_{11}\alpha_1 + Q_{12}\alpha_2) = \frac{V_f V_m (Q_{12f} - Q_{12m})(Q_{12f}\alpha_{1f} + Q_{22f}\alpha_{2f} - Q_{12m}\alpha_m - Q_{22m}\alpha_m)}{Q_{22m}V_f + Q_{22f}V_m}$$
$$- [(Q_{11f}\alpha_{1f} + Q_{12f}\alpha_{2f})V_f + (Q_{11m}\alpha_m + Q_{12m}\alpha_m)V_m]$$

Let $V_m = 1 - V_f$ and eliminate minus sign in both sides,

$$Q_{11}\alpha_1 + Q_{12}\alpha_2 = \frac{(V_f - V_f^2)(Q_{12m} - Q_{12f})(Q_{12f}\alpha_{1f} + Q_{22f}\alpha_{2f} - Q_{12m}\alpha_m - Q_{22m}\alpha_m)}{(Q_{22m} - Q_{22f})V_f + Q_{22f}}$$
$$+ (Q_{11f}\alpha_{1f} + Q_{12f}\alpha_{2f} - Q_{11m}\alpha_m - Q_{12m}\alpha_m)V_f + (Q_{11m}\alpha_m + Q_{12m}\alpha_m) \tag{2.28}$$

Let assume the above equation into this form in order to simplify,

$$Q_{11}\alpha_1 + Q_{12}\alpha_2 = C_1 \tag{2.29}$$

Similarly, the stress in 2-direction can be obtained as

$$\sigma_2 = Q_{12}\varepsilon_1^T + Q_{22}\varepsilon_2^T - (Q_{12}\alpha_1 + Q_{22}\alpha_2)\Delta T \tag{2.30}$$

From Equation (2.13),

$$\sigma_2 = Q_{12f}\varepsilon_1^T + Q_{22f}\varepsilon_{2f}^T - (Q_{12f}\alpha_{1f} + Q_{22f}\alpha_{2f})\Delta T$$

Substitute ε_{2f}^T into Equation (2.13) and rearrange it into the terms of ε_1^T, ε_2^T and ΔT.

$$\begin{aligned}\sigma_2 = {} & \frac{Q_{12f}Q_{22m}V_f + Q_{12m}Q_{22f}V_m}{Q_{22m}V_f + Q_{22f}V_m}\varepsilon_1^T + \frac{Q_{22f}Q_{22m}}{Q_{22m}V_f + Q_{22f}V_m}\varepsilon_2^T \\ & + [\frac{Q_{22f}V_m(Q_{12f}\alpha_{1f} + Q_{22f}\alpha_{2f} - Q_{12m}\alpha_m - Q_{22m}\alpha_m)}{Q_{22m}V_f + Q_{22f}V_m} - (Q_{12f}\alpha_{1f} + Q_{22f}\alpha_{2f})]\Delta T\end{aligned} \tag{2.31}$$

Equating (2.30) and (2.31), Q_{22} can be obtained as

$$Q_{22} = \frac{Q_{22f}Q_{22m}}{(Q_{22m} - Q_{22f})V_f + Q_{22f}} \tag{2.32}$$

The thermal related terms are obtained as

$$\begin{aligned}-(Q_{12}\alpha_1 + Q_{22}\alpha_2) = {} & \frac{Q_{22f}V_m(Q_{12f}\alpha_{1f} + Q_{22f}\alpha_{2f} - Q_{12m}\alpha_m - Q_{22m}\alpha_m)}{Q_{22m}V_f + Q_{22f}V_m} \\ & - (Q_{12f}\alpha_{1f} + Q_{22f}\alpha_{2f})\end{aligned}$$

Let $V_m = 1 - V_f$ and eliminate minus sign in both sides,

$$\begin{aligned}Q_{12}\alpha_1 + Q_{22}\alpha_2 = {} & \frac{Q_{22f}(Q_{12f}\alpha_{1f} + Q_{22f}\alpha_{2f} - Q_{12m}\alpha_m - Q_{22m}\alpha_m)(V_f - 1)}{(Q_{22m} - Q_{22f})V_f + Q_{22f}} \\ & + Q_{12f}\alpha_{1f} + Q_{22f}\alpha_{2f}\end{aligned} \tag{2.33}$$

Let assume the above equation into this form in order to simplify,

$$Q_{12}\alpha_1 + Q_{22}\alpha_2 = C_2 \tag{2.34}$$

The coefficient of thermal expansion, α_1 and α_2, are obtained by solving Equation (2.29) and (2.34).

$$\alpha_1 = \frac{Q_{22}C_1 - Q_{12}C_2}{Q_{11}Q_{22} - Q_{12}^2} \tag{2.35}$$

$$\alpha_2 = \frac{Q_{11}C_2 - Q_{12}C_1}{Q_{11}Q_{22} - Q_{12}^2} \tag{2.36}$$

The corresponding shear stress is given as

$$\tau_{12} = Q_{66}\gamma_{12} \tag{2.37}$$

Using (2.15),

$$\tau_{12f} = Q_{66f}\gamma_{12f}$$

Substituting γ_{12f} from (2.23), the τ_{12f} can be obtained in term of γ_{12}.

$$\tau_{12f} = \frac{Q_{66f}Q_{66m}}{Q_{66m}V_f + Q_{66f}V_m}\gamma_{12} \tag{2.38}$$

Equating (2.37) and (2.38), Q_{66} can be obtained as

$$Q_{66} = \frac{Q_{66f}Q_{66m}}{(Q_{66m} - Q_{66f})V_f + Q_{66f}} \tag{2.39}$$

The reduced stiffness matrix, $[Q]$, of the fiber and matrix constituents is given as

$$Q_{11f} = \frac{E_{1f}}{1 - v_{12f}v_{21f}} \tag{2.40}$$

$$Q_{12f} = \frac{E_{1f}v_{21f}}{1 - v_{12f}v_{21f}} \tag{2.41}$$

$$Q_{22f} = \frac{E_{2f}}{1 - v_{12f}v_{21f}} \tag{2.42}$$

$$Q_{66f} = G_{12f} \tag{2.43}$$

$$Q_{11m} = \frac{E_m}{1 - v_m^2} \tag{2.44}$$

$$Q_{12m} = \frac{E_m v_m}{1 - v_m^2} \tag{2.45}$$

$$Q_{22m} = \frac{E_m}{1 - v_m^2} \tag{2.46}$$

$$Q_{66m} = G_{12m} \tag{2.47}$$

2.3 Laminate Stiffness and Thermal Resultant Matrices

The laminate stiffness matrices, $[A]$, $[B]$, and $[D]$ can be obtained by integrating the reduced stiffness matrix, $[Q]$, through the thickness of the unit cell layer. For the integration, the component of $[Q]$ from Equation (2.26), (2.27), (2.32) and (2.34) are referred. The expressions of the components of these matrices are shown as below.

$$A_{11} = \int_{-h/2}^{h/2} Q_{11}\, dz = \int_{-h/2}^{-a} Q_{11}\, dz + \int_{-a}^{a} Q_{11}\, dz + \int_{a}^{h/2} Q_{11}\, dz$$

$$A_{11} = Q_{11m}h + (Q_{11f} - Q_{11m})I_1 - (Q_{12m} - Q_{12f})^2(I_5 - I_6) \tag{2.48}$$

$$A_{12} = \int_{-h/2}^{h/2} Q_{12}\, dz = Q_{12m}(h-2a) + (Q_{12f}Q_{22m} - Q_{12m}Q_{22f})I_5 + Q_{12m}Q_{22f}I_4 \tag{2.49}$$

$$A_{22} = \int_{-h/2}^{h/2} Q_{22}\, dz = Q_{22m}(h-2a) + Q_{22m}Q_{22f}I_4 \tag{2.50}$$

$$A_{66} = \int_{-h/2}^{h/2} Q_{66}\, dz = Q_{66m}(h-2a) + Q_{66m}Q_{66f}{I_4}^* \tag{2.51}$$

As expected,

$$A_{16} = \int_{-h/2}^{h/2} Q_{16}\, dz = 0 \tag{2.52}$$

$$A_{26} = \int_{-h/2}^{h/2} Q_{26}\, dz = 0 \tag{2.53}$$

$$B_{11} = \int_{-h/2}^{h/2} Q_{11}z\, dz = 0 \tag{2.54}$$

$$B_{12} = \int_{-h/2}^{h/2} Q_{12}z\, dz = 0 \tag{2.55}$$

$$B_{22} = \int_{-h/2}^{h/2} Q_{22}z\, dz = 0 \tag{2.56}$$

$$B_{66} = \int_{-h/2}^{h/2} Q_{66}z\, dz = 0 \tag{2.57}$$

$$B_{16} = \int_{-h/2}^{h/2} Q_{16}z\, dz = 0 \tag{2.58}$$

$$B_{26} = \int_{-h/2}^{h/2} Q_{26} z \, dz = 0 \tag{2.59}$$

$$D_{11} = \int_{-h/2}^{h/2} Q_{11} z^2 \, dz = \int_{-h/2}^{-a} Q_{11} z^2 \, dz + \int_{-a}^{a} Q_{11} z^2 \, dz + \int_{a}^{h/2} Q_{11} z^2 \, dz$$

$$D_{11} = Q_{11m} \frac{h^3}{12} + (Q_{11f} - Q_{11m}) I_{13} - (Q_{12m} - Q_{12f})^2 (I_{15} - I_{16}) \tag{2.60}$$

$$D_{12} = \int_{-h/2}^{h/2} Q_{12} z^2 \, dz = Q_{12m} (\frac{h^3}{12} - \frac{2a^3}{3}) + (Q_{12f} Q_{22m} - Q_{12m} Q_{22f}) I_{15} + Q_{12m} Q_{22f} I_{14} \tag{2.61}$$

$$D_{22} = \int_{-h/2}^{h/2} Q_{22} z^2 \, dz = Q_{22m} (\frac{h^3}{12} - \frac{2a^3}{3}) + Q_{22m} Q_{22f} I_{14} \tag{2.62}$$

$$D_{66} = \int_{-h/2}^{h/2} Q_{66} z^2 \, dz = Q_{66m} (\frac{h^3}{12} - \frac{2a^3}{3}) + Q_{66m} Q_{66f} {I_{14}}^* \tag{2.63}$$

$$D_{16} = \int_{-h/2}^{h/2} Q_{16} z^2 \, dz = 0 \tag{2.64}$$

$$D_{26} = \int_{-h/2}^{h/2} Q_{26} z^2 \, dz = 0 \tag{2.65}$$

Where the list of I parameters are provided in Appendix A.

The thermal resultant and moment matrices, $[N^t]$ and $[M^t]$, can be obtained by integrating the constitutive equation of the unit cell layer. The procedure and expression of the thermal resultant matrices are shown as below.

The constitutes equation of the unit cell layer,

$$[\sigma]_{1,2} = [Q]_{1,2}[\varepsilon^T]_{1,2} - [Q]_{1,2}[\alpha]_{1,2}\Delta T$$

From $[\varepsilon^T]_{1,2} = [\varepsilon^0]_{1,2} + z[k]_{1,2}$

$$[\sigma]_{1,2} = [Q]_{1,2}[\varepsilon^0]_{1,2} + z[Q]_{1,2}[k]_{1,2} - [Q]_{1,2}[\alpha]_{1,2}\Delta T \tag{2.66}$$

Integration of the stresses from Equation (2.66) across the all thickness in laminate gives the force resultants:

$$[N]_{1,2} = \int_{-h/2}^{h/2} [\sigma]_{1,2}\, dz$$

$$[N]_{1,2} = \int_{-h/2}^{h/2} \left\{[Q]_{1,2}[\varepsilon^0]_{1,2} + z[Q]_{1,2}[k]_{1,2} - [Q]_{1,2}[\alpha]_{1,2}\Delta T\right\}\, dz$$

$$[N]_{1,2} = [A]_{1,2}[\varepsilon^0]_{1,2} + [B]_{1,2}[k]_{1,2} - [N^t]_{1,2} \tag{2.67}$$

Therefore, the themal resultant matrix is obtained.

$$[N^t]_{1,2} = \int_{-h/2}^{h/2} [Q]_{1,2}[\alpha]_{1,2}\Delta T\, dz$$

or, in view,

$$\begin{bmatrix} N_1^t \\ N_2^t \\ N_{12}^t \end{bmatrix} = \int_{-h/2}^{h/2} \left\{ \begin{bmatrix} Q_{11} & Q_{12} & 0 \\ Q_{12} & Q_{22} & 0 \\ 0 & 0 & Q_{66} \end{bmatrix} \begin{bmatrix} \alpha_1 \Delta T \\ \alpha_2 \Delta T \\ 0 \end{bmatrix} \right\} dz \tag{2.68}$$

First, the thermal resultant in 1-direction is considered.

$$N_1^t = \int_{-h/2}^{h/2} \{Q_{11}\alpha_1\Delta T + Q_{12}\alpha_2\Delta T\}\, dz$$

$$N_1^t = \Delta T \int_{-h/2}^{h/2} \left\{ Q_{11}\frac{Q_{22}C_1 - Q_{12}C_2}{Q_{11}Q_{22} - Q_{12}^2} + Q_{12}\frac{Q_{11}C_2 - Q_{12}C_1}{Q_{11}Q_{22} - Q_{12}^2} \right\} dz$$

$$N_1^t = \Delta T \int_{-h/2}^{h/2} \left\{ \frac{Q_{11}Q_{22}C_1 - Q_{11}Q_{12}C_2 + Q_{11}Q_{12}C_2 - Q_{12}^2C_1}{Q_{11}Q_{22} - Q_{12}^2} \right\} dz$$

$$N_1^t = \Delta T \int_{-h/2}^{h/2} \left\{ \frac{Q_{11}Q_{22} - Q_{12}^2}{Q_{11}Q_{22} - Q_{12}^2}C_1 \right\} dz$$

Where, C_1 is from Equation (2.28) and (2.29).

$$C_1 = \frac{(V_f - V_f^2)(Q_{12m} - Q_{12f})(Q_{12f}\alpha_{1f} + Q_{22f}\alpha_{2f} - Q_{12m}\alpha_m - Q_{22m}\alpha_m)}{(Q_{22m} - Q_{22f})V_f + Q_{22f}}$$
$$+ (Q_{11f}\alpha_{1f} + Q_{12f}\alpha_{2f} - Q_{11m}\alpha_m - Q_{12m}\alpha_m)V_f + (Q_{11m}\alpha_m + Q_{12m}\alpha_m)$$

Therefore,

$$N_1^t = \Delta T \int_{-h/2}^{h/2} C_1\, dz = \Delta T \left\{ \int_{-h/2}^{-a} C_1\, dz + \int_{-a}^{a} C_1\, dz + \int_{a}^{h/2} C_1\, dz \right\}$$

$$N_1^t = \Delta T[(Q_{11m}\alpha_m + Q_{12m}\alpha_m)h + (Q_{11f}\alpha_{1f} + Q_{12f}\alpha_{2f} - Q_{11m}\alpha_m - Q_{12m}\alpha_m)I_1$$
$$+ (Q_{12m} - Q_{12f})(Q_{12f}\alpha_{1f} + Q_{22f}\alpha_{2f} - Q_{12m}\alpha_m - Q_{22m}\alpha_m)(I_5 - I_6)] \tag{2.69}$$

Then, the thermal resultant in 2-direction is considered.

$$N_2^t = \int_{-h/2}^{h/2} \{Q_{12}\alpha_1\Delta T + Q_{22}\alpha_2\Delta T\}\, dz$$

$$N_2^t = \Delta T \int_{-h/2}^{h/2} \left\{ Q_{12}\frac{Q_{22}C_1 - Q_{12}C_2}{Q_{11}Q_{22} - Q_{12}^2} + Q_{22}\frac{Q_{11}C_2 - Q_{12}C_1}{Q_{11}Q_{22} - Q_{12}^2} \right\} dz$$

$$N_2^t = \Delta T \int_{-h/2}^{h/2} \left\{ \frac{Q_{12}Q_{22}C_1 - Q_{12}^2C_2 + Q_{11}Q_{22}C_2 - Q_{12}Q_{22}C_1}{Q_{11}Q_{22} - Q_{12}^2} \right\} dz$$

$$N_2^t = \Delta T \int_{-h/2}^{h/2} \left\{ \frac{Q_{11}Q_{22} - Q_{12}^2}{Q_{11}Q_{22} - Q_{12}^2}C_2 \right\} dz$$

Where, C_2 is from (2.33) and (2.34).

$$C_2 = \frac{Q_{22f}(Q_{12f}\alpha_{1f} + Q_{22f}\alpha_{2f} - Q_{12m}\alpha_m - Q_{22m}\alpha_m)(V_f - 1)}{(Q_{22m} - Q_{22f})V_f + Q_{22f}} + Q_{12f}\alpha_{1f} + Q_{22f}\alpha_{2f}$$

Therefore,

$$N_2^t = \Delta T \int_{-h/2}^{h/2} C_2\, dz = \Delta T \left\{ \int_{-h/2}^{-a} C_2\, dz + \int_{-a}^{a} C_2\, dz + \int_{a}^{h/2} C_2\, dz \right\}$$

$$N_2^t = \Delta T[(Q_{12f}\alpha_{1f} + Q_{22f}\alpha_{2f})h - (Q_{12f}\alpha_{1f} + Q_{22f}\alpha_{2f} - Q_{12m}\alpha_m - Q_{22m}\alpha_m)(h - 2a) + Q_{22f}(Q_{12f}\alpha_{1f} + Q_{22f}\alpha_{2f} - Q_{12m}\alpha_m - Q_{22m}\alpha_m)(I_5 - I_4)] \tag{2.70}$$

Integration of the stresses and height from Equation (2.66) across the all thickness in laminate gives the thermal moment:

$$[M]_{1,2} = \int_{-h/2}^{h/2} z[\sigma]_{1,2}\, dz$$

Therefore,

$$[M]_{1,2} = \int_{-h/2}^{h/2} \left\{ z[Q]_{1,2}[\varepsilon^0]_{1,2} + z^2[Q]_{1,2}[k]_{1,2} - z[Q]_{1,2}[\alpha]_{1,2}\Delta T \right\} dz$$

$$[M]_{1,2} = [B]_{1,2}[\varepsilon^0]_{1,2} + [D]_{1,2}[k]_{1,2} - [M^t]_{1,2} \tag{2.71}$$

Therefore, the themal moment matrix is obtained.

$$[M^t]_{1,2} = \int_{-h/2}^{h/2} z[Q]_{1,2}[\alpha]_{1,2}\Delta T\, dz$$

or, in view,

$$\begin{bmatrix} M_1^t \\ M_2^t \\ M_{12}^t \end{bmatrix} = \int_{-h/2}^{h/2} \left\{ z \begin{bmatrix} Q_{11} & Q_{12} & 0 \\ Q_{12} & Q_{22} & 0 \\ 0 & 0 & Q_{66} \end{bmatrix} \begin{bmatrix} \alpha_1 \Delta T \\ \alpha_2 \Delta T \\ 0 \end{bmatrix} \right\} dz \tag{2.72}$$

With the same way that is used to get the thermal resultant matrix, the thermal moment matrix is obtained.

$$M_1^t = \Delta T \int_{-h/2}^{h/2} zC_1\, dz = 0 \tag{2.73}$$

$$M_2^t = \Delta T \int_{-h/2}^{h/2} z C_2 \, dz = 0 \tag{2.74}$$

As expected, $[M^t] = 0$

2.4 Methods of Obtaining the Effective Properties

The laminate compliances matrices, $[a]$, $[b]$, $[b]^T$ and $[d]$, can be obtained from the inversion of the laminate stiffness matrices, $[A]$, $[B]$, and $[D]$, as shown below.

$$\begin{bmatrix} a & b \\ b^T & d \end{bmatrix} = \begin{bmatrix} A & B \\ B & D \end{bmatrix}^{-1} \tag{2.75}$$

The effective moduli of the laminates can be obtained by the extensional laminate compliance matrix, $[a]$, and the entire unit cell thichness, t, as shown below.

$$\bar{E}_1 = \frac{1}{a_{11} t} \tag{2.76}$$

$$\bar{E}_2 = \frac{1}{a_{22} t} \tag{2.77}$$

For a symmetric and banlanced laminate, the coupling stiffness matrix, $[B]$, will be zero that make the coupling compliance matrices, $[b]$ and $[b]^T$ go to zero, . With this condition, the effective moduli of the laminate can be directly get from the laminate stiffness matrix, $[A]$, as listed below.

$$\bar{E}_1 = (A_{11} - \frac{A_{12}^2}{A_{22}}) \frac{1}{t} \tag{2.78}$$

$$\bar{E}_2 = (A_{22} - \frac{A_{12}^2}{A_{11}}) \frac{1}{t} \tag{2.79}$$

To get the coefficients of thermal expansion, α_1 and α_2, the mid plane strain, ε_1 and ε_2, need to be obtained by assume no external force and moment in Equation (2.67) and (2.71).

Considering (2.67) without mechanical force, we have

$$[N^t]_{1,2} = [A]_{1,2}[\varepsilon^0]_{1,2} + [B]_{1,2}[k]_{1,2} \tag{2.80}$$

From $[B] = 0$,

$$[N^t]_{1,2} = [A]_{1,2}[\varepsilon^0]_{1,2}$$

Inverse the above equation.

$$[\varepsilon^0]_{1,2} = [a]_{1,2}[N^t]_{1,2} \tag{2.81}$$

$$\begin{bmatrix} \varepsilon_1^0 \\ \varepsilon_2^0 \\ \gamma_{12}^0 \end{bmatrix} = \begin{bmatrix} a_{11} & a_{12} & 0 \\ a_{12} & a_{22} & 0 \\ 0 & 0 & a_{66} \end{bmatrix} \begin{bmatrix} N_1^t \\ N_2^t \\ 0 \end{bmatrix} \tag{2.82}$$

Therefore,

$$\varepsilon_1^0 = a_{11}N_1^t + a_{12}N_2^t \tag{2.83}$$

$$\varepsilon_2^0 = a_{12}N_1^t + a_{22}N_2^t \tag{2.84}$$

$$\gamma_{12}^0 = 0 \tag{2.85}$$

Then, consider Equation (2.70) without extenal moment.

$$0 = [B]_{1,2}[\varepsilon^0]_{1,2} + [D]_{1,2}[k]_{1,2} - [M^t]_{1,2}$$

$$[M^t]_{1,2} = [B]_{1,2}[\varepsilon^0]_{1,2} + [D]_{1,2}[k]_{1,2} \tag{2.86}$$

From $[M^t]_{1,2} = 0$ and $[B]_{1,2} = 0$,

$$[D]_{1,2}[k]_{1,2} = 0$$

$$[k]_{1,2} = 0 \tag{2.87}$$

From Equation (2.82) and (2.83), the coefficient of thermal expansion can be get in the below equation.

First, consider the longitudinal coefficient of thermal expansion.

$$\bar{\alpha}_1 \Delta T = \varepsilon_1^0 \tag{2.88}$$

Therefore,

$$\bar{\alpha}_1 = \frac{\varepsilon_1^0}{\Delta T} \tag{2.89}$$

Do the same approach for the transverse coefficient of thermal expansion. Thus,

$$\bar{\alpha}_2 = \frac{\varepsilon_2^0}{\Delta T} \tag{2.90}$$

2.5 Stresses Components due to Thermal Expansion

With this present solution, the stress components of the fiber and matrix can also be estimated by any given z position. From Equation (2.8), the fiber volume fraction in each layer can be obtained with the z position.

$$V_f = \begin{cases} 0 & z \in [\frac{-h}{2}, -a] \cup [a, \frac{h}{2}] \\ \frac{w_i}{W} = \frac{2b}{W}\sqrt{1 - \frac{z^2}{a^2}} & z \in [-a, a] \end{cases}$$

The stress, σ_{1f} and σ_{1m} of a given sublayer can be obtained from Equations (2.9) and (2.10).

$$\sigma_{1f} = Q_{11f}\varepsilon_1^T + Q_{12f}\varepsilon_{2f}^T - (Q_{11f}\alpha_{1f} + Q_{12f}\alpha_{2f})\Delta T$$

$$\sigma_{1m} = Q_{11m}\varepsilon_1^T + Q_{12m}\varepsilon_{2m}^T - (Q_{11m}\alpha_m + Q_{12m}\alpha_m)\Delta T$$

Where ε_1^T, ε_{2f}^T and ε_{2m}^T are given in Equations (2.21) and (2.22).

σ_{2f} and σ_{2m} of the given sublayer is shown in Equations (2.17) and (2.18). It should be noted that $\gamma_{12} \equiv 0$ resulting in $\tau_{12} = \tau_{12f} = \tau_{12m} = 0$.

2.6 Rule-of-Mixture and Schapery's Methods

Rule of Mixture is a conventional method to estimate the properties of composite material, based on the properties and volume fraction of each constituent. The effective moduli and the coefficients of thermal expansion from the Rule of Mixture are expressed as below equations.

For the longitudinal modulus,

$$E_1 = E_{1f}V_f + E_mV_m \tag{2.91}$$

For the transverse modulus,

$$\frac{1}{E_2} = \frac{V_f}{E_{2f}} + \frac{V_m}{E_m} \tag{2.92}$$

For Poissons ratio,

$$v_{12} = v_{12f}V_f + v_{12m}V_m \tag{2.93}$$

For the shear modulus,

$$\frac{1}{G_{12}} = \frac{V_f}{G_{12f}} + \frac{V_m}{G_m} \tag{2.94}$$

Unlike the effective moduli, CTE's does not follow the ROM.

The coefficient of thermal expansion in the longitudinal direction (along the fiber) is given as [12],

$$\alpha_1 = \frac{E_{1f}\alpha_{1f}V_f + E_{1m}\alpha_mV_m}{E_{1f}V_f + E_{1m}V_m} \tag{2.95}$$

The coefficient of thermal expansion in the transverse direction (perpendicular to the fiber) for isotropic and orthotropic is given as [3],

For the isotropic fiber,

$$\alpha_2 = \alpha_fV_f(1 + v_f) + \alpha_mV_m(1 + v_m) - v_{12}\alpha_1 \tag{2.96}$$

For the orthotropic fiber,

$$\alpha_2 = \alpha_{2f} V_f (1 + v_{12f} \frac{\alpha_{1f}}{\alpha_{2f}}) + \alpha_m V_m (1 + v_m) - v_{12} \alpha_1 \tag{2.97}$$

CHAPTER 3

FINITE ELEMENT ANALYSIS

The finite element model of a unit cell of composite lamina is created to calculate the effective moduli and coefficients of thermal expansion. A three-dimensional finite element model is developed in this chapter using ANSYS 11.0 program. The ANSYS codes are listed in Appendix B. In order to verify the model, the isotropic material properties are first applied in each model before applying to composite material. The difference of results in the calculated case and materials properties is less than 0.1%.

3.1 Finite Element Model for Longitudinal Load

3.1.1 Geometric Description

Both circular and elliptical configurations cross-sections of fiber are chosen for study. Figure 3.1 and 3.2 show the description of the unit cell geometries used in this study.

In fiber volume fraction study, the fiber volume fraction, V_f, is independent variable. Due to the square array model, the width and height, W and h, are fixed at 0.005 inch. The radius, r, that is the dependent variable can be calculated from the fiber volume fraction and the width of the unit cell. For elliptical cross-section of fiber, V_f and a (the semi-major axis) are given, then b (the semi-minor axis) is determined. The length of model of unit cell is 10 times of the width.

3.1.2 Materials Used

The fiber reinforced composite is consisted of two portions, fiber and matrix, which are E-glass and Epoxy 3501-6, respectively. The data of materials properties are given in Daniel and Ishai[12].

The orthotropic material properties of the fiber, E-glass, are shown below.

$E_{11} = 10.5 \times 10^6\ psi$, $E_{22} = 10.5 \times 10^6\ psi$, $E_{33} = 10.5 \times 10^6\ psi$

$v_{12} = 0.23$, $v_{23} = 0.23$, $v_{13} = 0.23$

$G_{12} = 4.3 \times 10^6\ psi$, $G_{23} = 4.3 \times 10^6\ psi$, $G_{13} = 4.3 \times 10^6\ psi$

$\alpha_1 = 2.8 \times 10^{-6}/\,^\circ\mathrm{F}$, $\alpha_2 = 2.8 \times 10^{-6}/\,^\circ\mathrm{F}$, $\alpha_3 = 2.8 \times 10^{-6}/\,^\circ\mathrm{F}$

Then, the isotropic material properties of the matrix, Epoxy 3501-6, are shown below.

$E = 0.62 \times 10^6\ psi$, $v = 0.35$, $G = 0.24 \times 10^6\ psi$

$\alpha = 25 \times 10^{-6}/\,^\circ\mathrm{F}$

Where the subscripts 1 refers to fiber direction, 2 is transverse to fiber direction and 3 is perpendicular to 1-2 plane. E_{11}, E_{22} and E_{33} are Youngs modulus in 1-2-3 coordinate. G_{12}, G_{23} and G_{13} are the shear modulus along the 1-2, 2-3 and 1-3 planes respectively. v_{12}, v_{23} and v_{13} are Poissons ratio.

3.1.3 Element Type Used

SHELL93 and SOLID95 of ANSYS 11.0 are chosen for the model. SHELL93 is an 8-node shell element with six degrees of freedom at each node. This element type is used only for 2D meshing in XZ plane. SOLID95 is a 20-node solid element with three degrees of freedom in each node. It is a higher order 3D in 20-node brick element.

3.1.4 Modeling and Mesh Generation

The modeling and mesh generation is done using ANSYS 11.0 preprocessor tool. The procedure used to develop a square array model is described below.

1. Define SHELL93 as element type 1 and SOLID95 as element type 2.

2. Define the material properties of E-glass as material model 1 and the material properties of Epoxy 3501-6 as material model 2.

3. Create the cross-sectional area of the square array with both circular and elliptical fiber of the unit cell fiber reinforced composite. The fiber volume fraction is given as 0.55 for this model. The fiber was drawn as the circular and elliptical configuration at the center and the matrix was placed in the rest area of that square. The quarter of cross sectional area is drawn firstly and then the whole one was created by reflecting the quarter model. In addition, the square was created in the corner of fiber and matrix area as in Figure 3.3 and 3.4 in order to get the finer mesh.

4. Mesh the cross sectional area in 2D as element type 1. The size of area mesh is about 0.1 of the width. The following explains each step and Figure 3.5 and 3.6 shows the 2D mesh.

- The fiber area is selected and meshed as material model 1 (E-glass).
- The matrix area is selected and meshed as material model 2 (Epoxy 3501-6).

5. Create the 3D element by extruding the 2D element along the x-axis. The below list explained in each step and Figure 3.7 and 3.8 shows the 3D mesh.

- The 2D fiber elements are selected and extruded along the x-axis as the element type 2 and the material model 1.
- The 2D matrix elements are selected and extrude along the x-axis as the element type 2 and the material model 2.

- The all 2D elements are deleted and the all 3D elements are merged all nodes.

3.1.5 Boundary and Loading Conditions

To determine the mechanical properties in this model, a mechanical load is applied. The yz-plane at the edge of the model is coupled to ensure the uniform deformation in x-direction because of the perfect bonding assumption. The corresponding boundary conditions are listed below.

1. All the nodes at x=0 are constrained along x-axis (loading axis) i.e. Ux=0.

2. All the nodes at y=0 are constrained along y-axis (loading axis) i.e. Uy=0.

3. All the nodes at z=0 are constrained along z-axis (loading axis) i.e. Uz=0.

4. All the nodes at end of the unit cell (x=L) are coupled along x-axis to get the uniform deformation in x-direction.

5.All the nodes at top and bottom of the unit cell in y-direction (y=W/2,-W/2) are coupled along y-axis to get the uniform deformation in y-direction.

6.All the nodes at top and bottom of the unit cell in z-direction (z=W/2,-W/2) are coupled along z-axis to get the uniform deformation in z-direction.

7. Apply the longitudinal load, $F_x = 1$, at $x = L$, $y = 0$ and $z = 0$.

3.2 Finite Element Model for Thermal Load

Due to the same configuration, material and element type, this model can use all steps in longitudinal load model except the boundary condition.

For thermal load application only, the boundary conditions of the model is different from the previous case.

3.2.1 Boundary and Loading Conditions

The boundary conditions of this model do not have the mechanical load because it was created to study the coefficient of thermal expansion. Hence, only uniform temperature was applied in all nodes. The list below shows all boundary conditions of this model.

1. All the nodes at x=0 are constrained along x-axis (loading axis) i.e. Ux=0.

2. All the nodes at y=0 are constrained along y-axis (loading axis) i.e. Uy=0.

3. All the nodes at z=0 are constrained along z-axis (loading axis) i.e. Uz=0.

4. All the nodes at end of the unit cell (x=L) are coupled along x-axis to get the uniform deformation in x-direction.

5.All the nodes at top and bottom of the unit cell in y-direction (y=W/2,-W/2) are coupled along y-axis to get the uniform deformation in y-direction.

6.All the nodes at top and bottom of the unit cell in z-direction (z=W/2,-W/2) are coupled along z-axis to get the uniform deformation in z-direction.

7. All nodes are added the temperature reference and the uniform temperature to get ΔT.

3.3 Finite Element Model for Transverse Load

3.3.1 Geometric Description

The model used in this case is not different from the previous case. To reduce the size of model, a shorter length of the model is used. The length in this model is only 0.1 of the width. Therefore, only the 3D mesh of this models are shown in Figure 3.9 and 3.10.

3.3.2 Boundary and Loading Conditions

Boundary conditions of this model are given below:

1. All the nodes at x=L/2 are constrained along x-axis (loading axis) i.e. Ux=0.

2. All the nodes at y=0 are constrained along y-axis (loading axis) i.e. Uy=0.

3. All the nodes at z=0 are constrained along z-axis (loading axis) i.e. Uz=0.

4. All the nodes at end of the unit cell (y=W/2) are coupled along x-axis to get the uniform deformation in x-direction.

5.All the nodes at top and bottom of the unit cell in x-direction (x=0,L) are coupled along y-axis to get the uniform deformation in y-direction.

6.All the nodes at top and bottom of the unit cell in z-direction (z=W/2,-w/2) are coupled along z-axis to get the uniform deformation in z-direction.

7. Apply the transverse load, $F_y = 1$, at $x = 0$, $y = W/2$ and $z = 0$.

3.4 Method of Obtaining the Effective Properties

The effective moduli, $\bar{E}_1$ and $\bar{E}_2$, and coefficients of thermal expansion, $\bar{\alpha}_1$ and $\bar{\alpha}_2$, can not be directly obtained from the finite element output. These properties can be calculated as described below.

For the longitudinal and transverse load models,

$$\bar{E}_1 = \frac{P_x}{A_x \varepsilon_x} \tag{3.1}$$

$$\bar{E}_2 = \frac{P_y}{A_y \varepsilon_y} \tag{3.2}$$

Where ε_x is the strain of the model in x-direction at $x = L$ and ε_y is the strain of this model in y-direction at $y = W/2$.

ε_x is directly obtained in finite element output like in Figure 3.11 and 3.12. Unlikely, ε_y has to be calculate from the deformation at $y = W/2$ over $W/2$ which is shown in Figure 3.13 and 3.14. P_x, P_y, A_x and A_y are the applied force and the areas of the model in the x- and y-directions (or yz- and xz-plane), respectively.

For the thermal load model,

$$\bar{\alpha}_1 = \frac{\varepsilon_x^T}{\Delta T} \tag{3.3}$$

$$\bar{\alpha}_2 = \frac{\varepsilon_y^T}{\Delta T} \tag{3.4}$$

Where ε_x^T is the total strain of the model in x-direction at $x = L$ and ε_y^T is the total strain of this model in y-direction at $y = W/2$ or $y = -W/2$.

ε_x^T is directily obtained in finite element output as in Figure 3.11 and 3.12. Unlikely, ε_y^T has to be calculate from the deformation at $y = W/2$ over $W/2$ which is also shown in Figure 3.13 and 3.14. ΔT is the difference between the reference and applied temperature which are applied in the model.

Moreover, the stresses components in x-direction due to the temperature effect are also directly obtained from FEM result. Figure 3.15 and 3.16 show the stress contour in FEM model. However, the stresses components can be obtained in the specific nodes.

With the symmetry model, the quarter model can be determined as the whole model. Therefore, the quarter FEM model is used to analyze in order to reduce the time consuming.

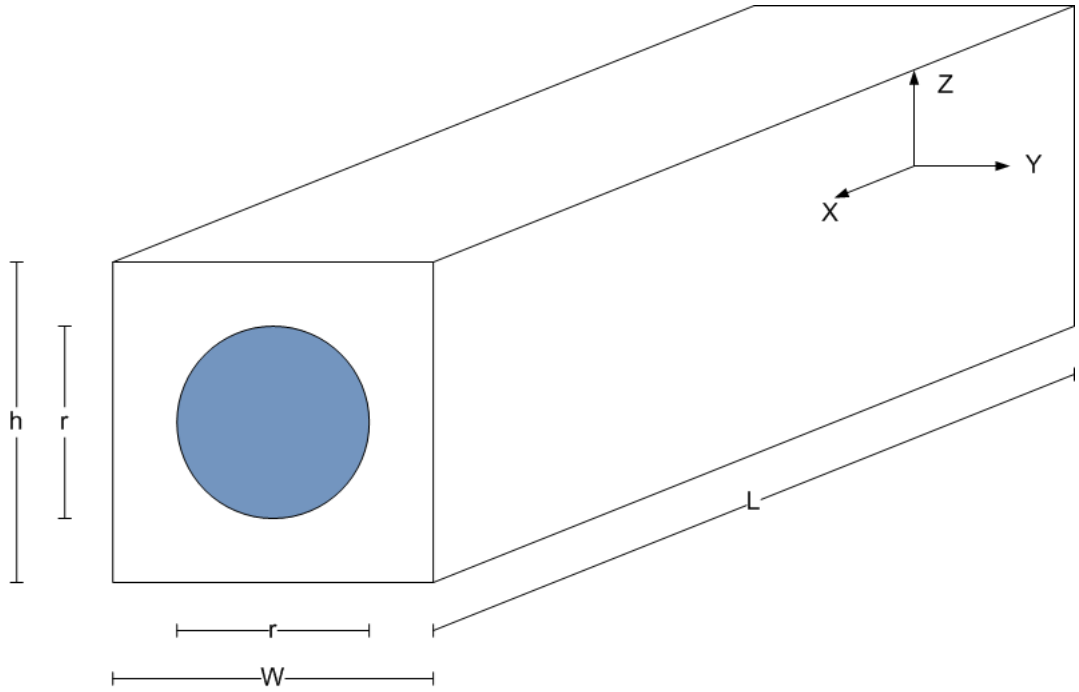

Figure 3.1. Unit Cell with Circular Fiber.

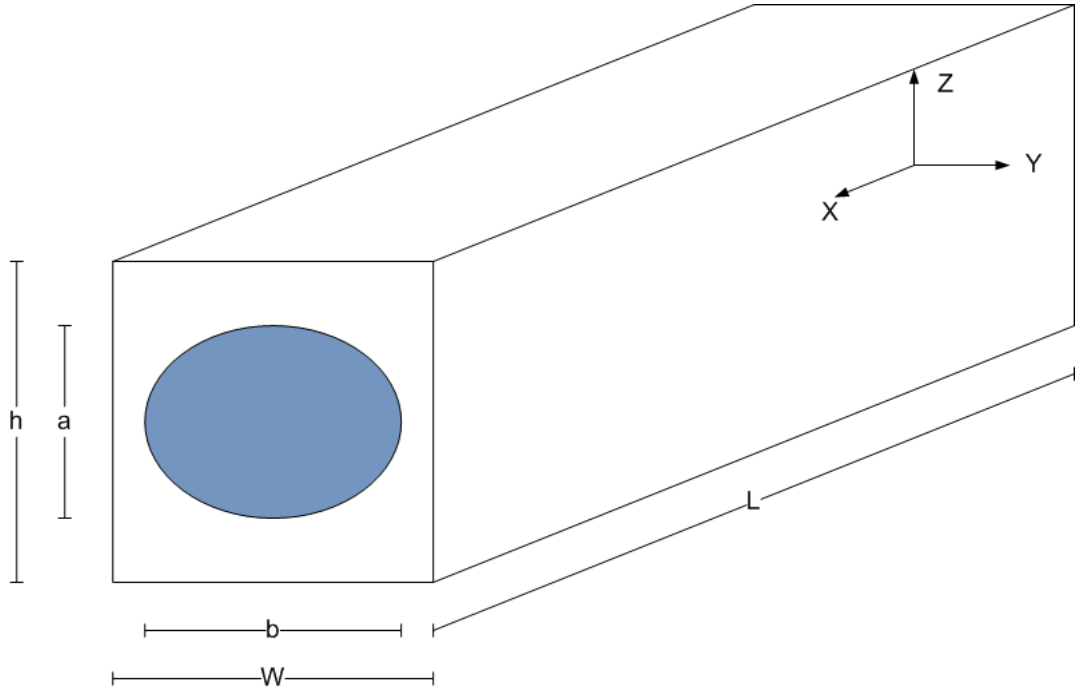

Figure 3.2. Unit Cell with Elliptical Fiber.

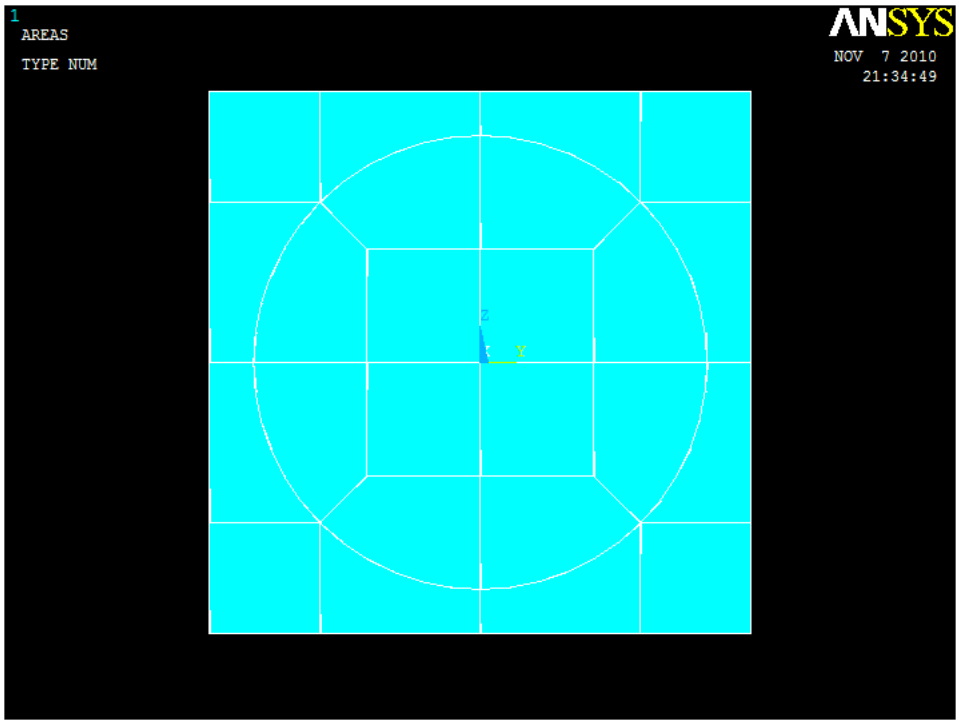

Figure 3.3. Cross-sectional Area in FEM Model with Circular Fiber.

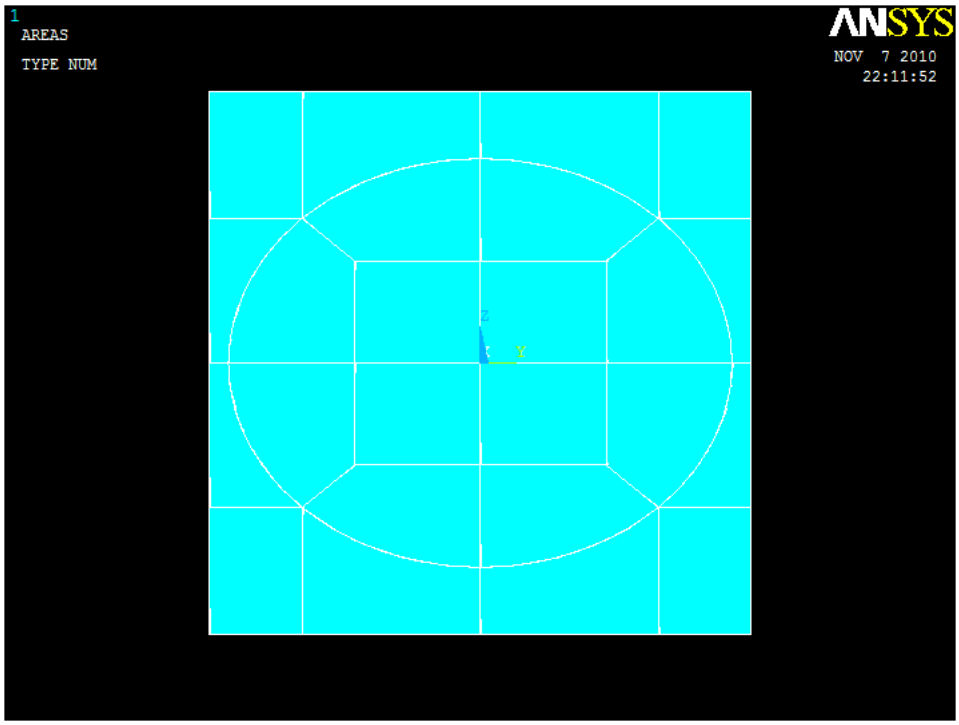

Figure 3.4. Cross-sectional Area in FEM Model with Elliptical Fiber.

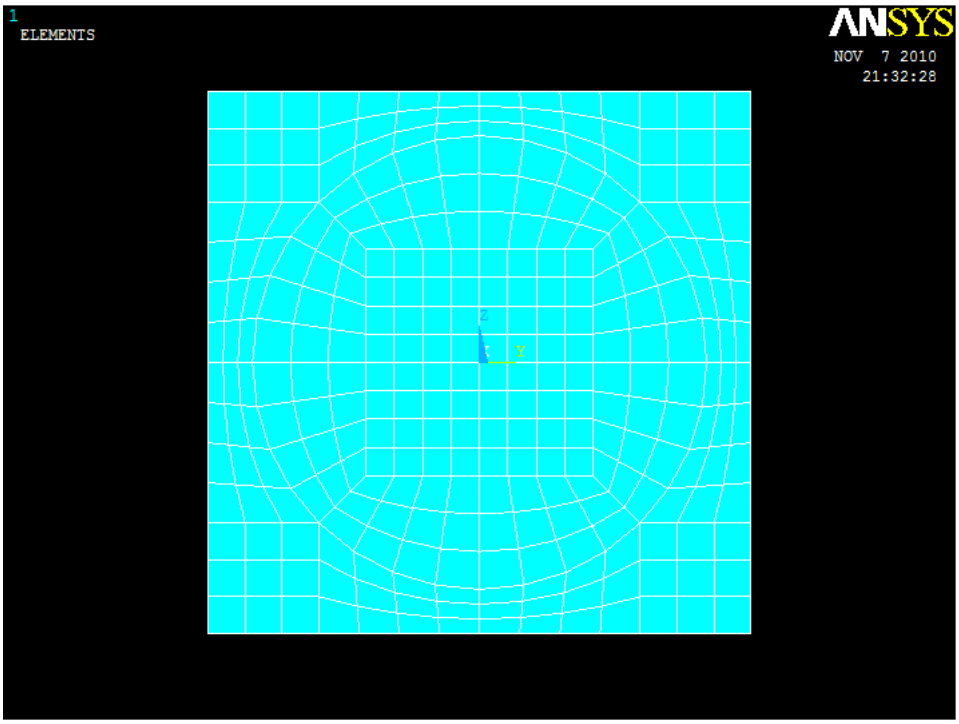

Figure 3.5. 2D-Mesh in FEM Model with Circular Fiber.

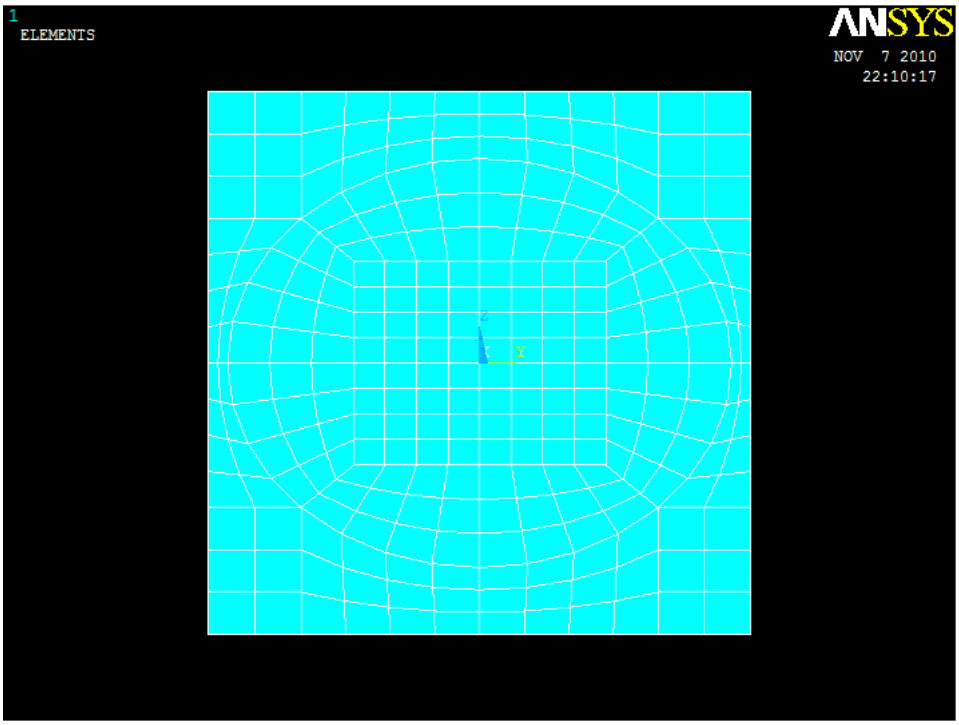

Figure 3.6. 2D-Mesh in FEM Model with Elliptical Fiber.

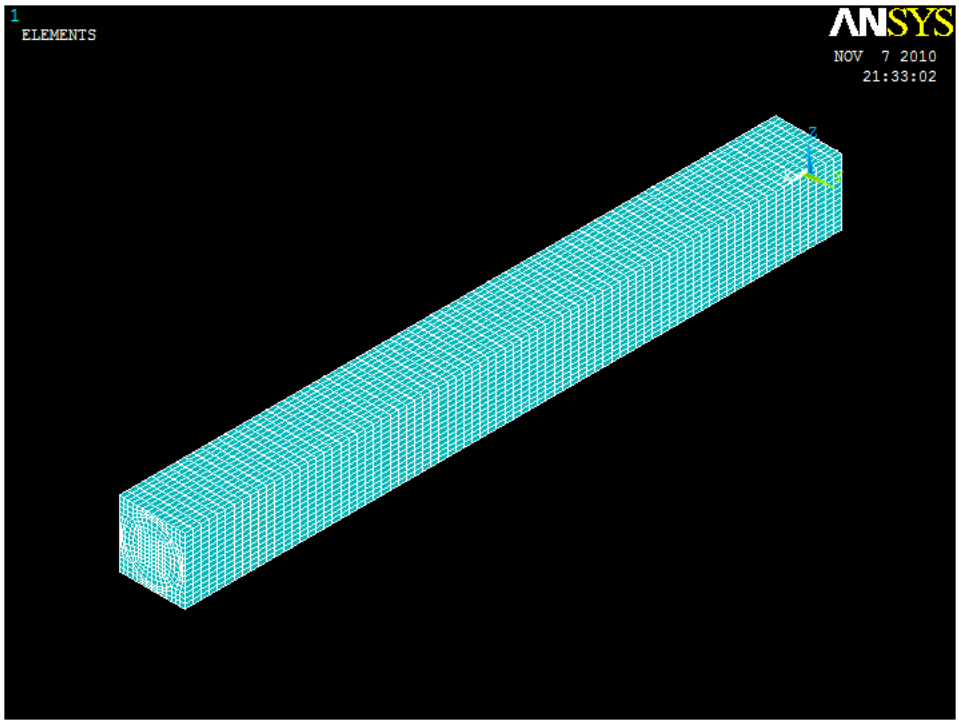

Figure 3.7. 3D-Mesh in FEM Model with Circular Fiber.

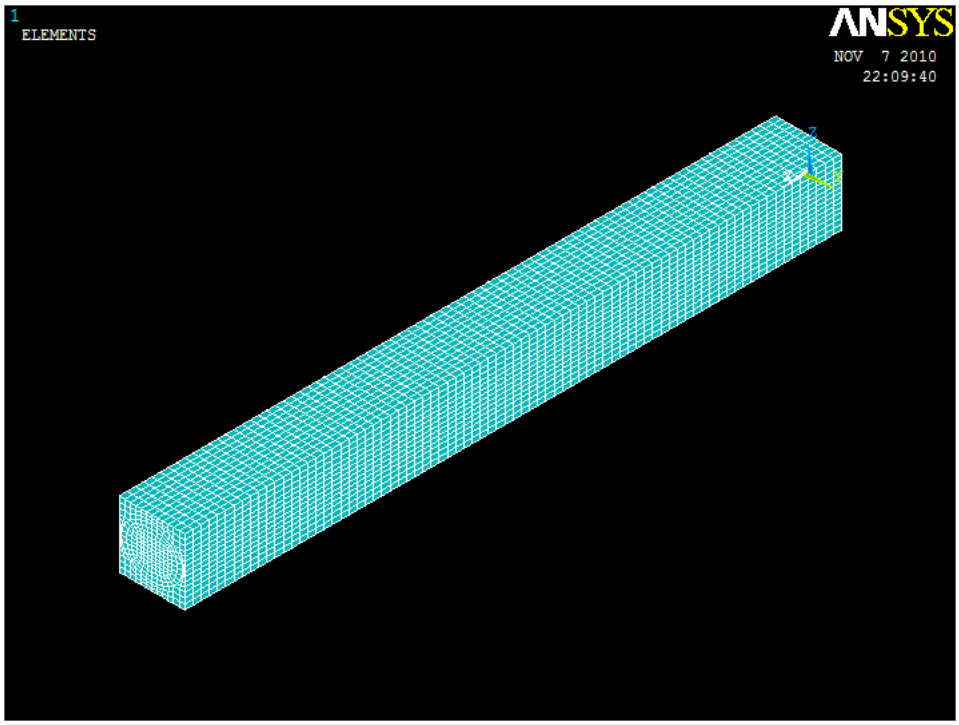

Figure 3.8. 3D-Mesh in FEM Model with Elliptical Fiber.

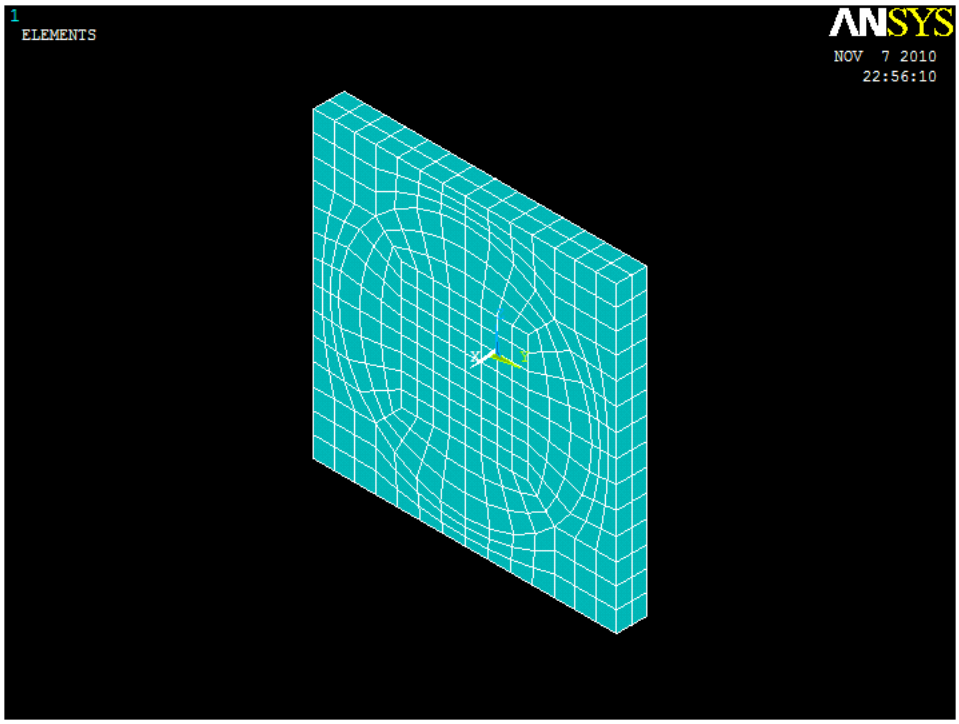

Figure 3.9. 3D-Mesh in Transverse Load Model with Circular Fiber.

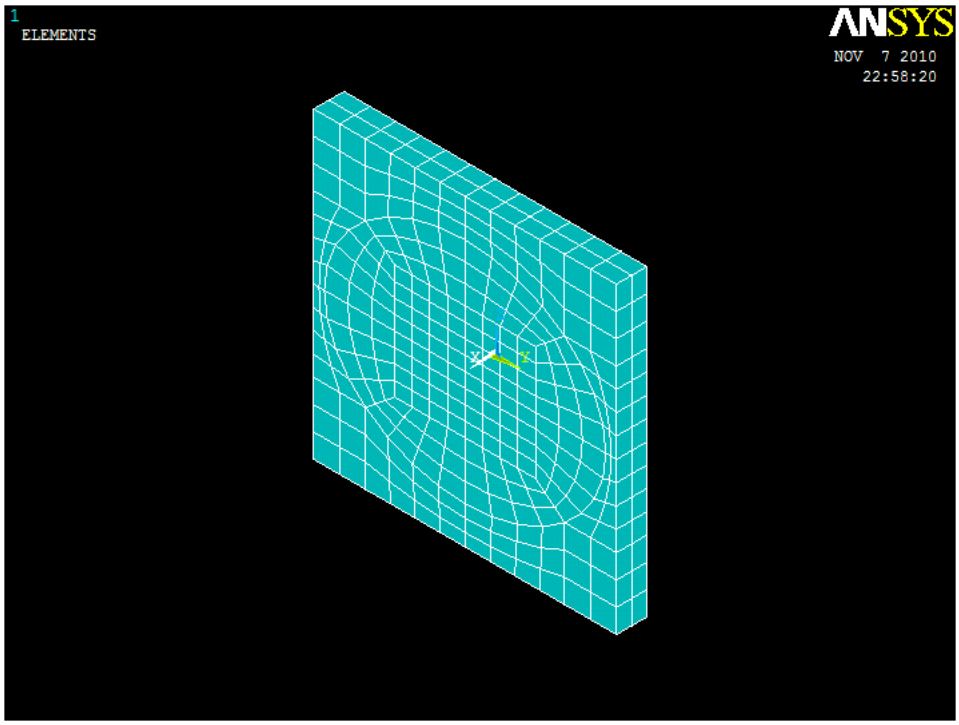

Figure 3.10. 3D-Mesh in Transverse Load Model with Elliptical Fiber.

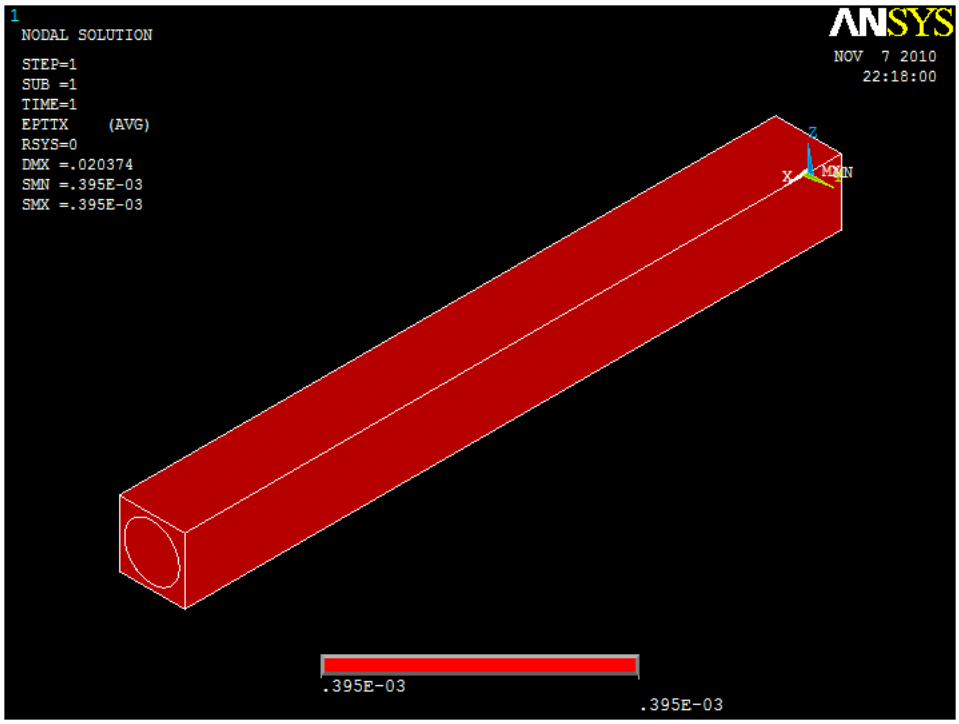

Figure 3.11. X-direction Total Strain in FEM Model with Circular Fiber.

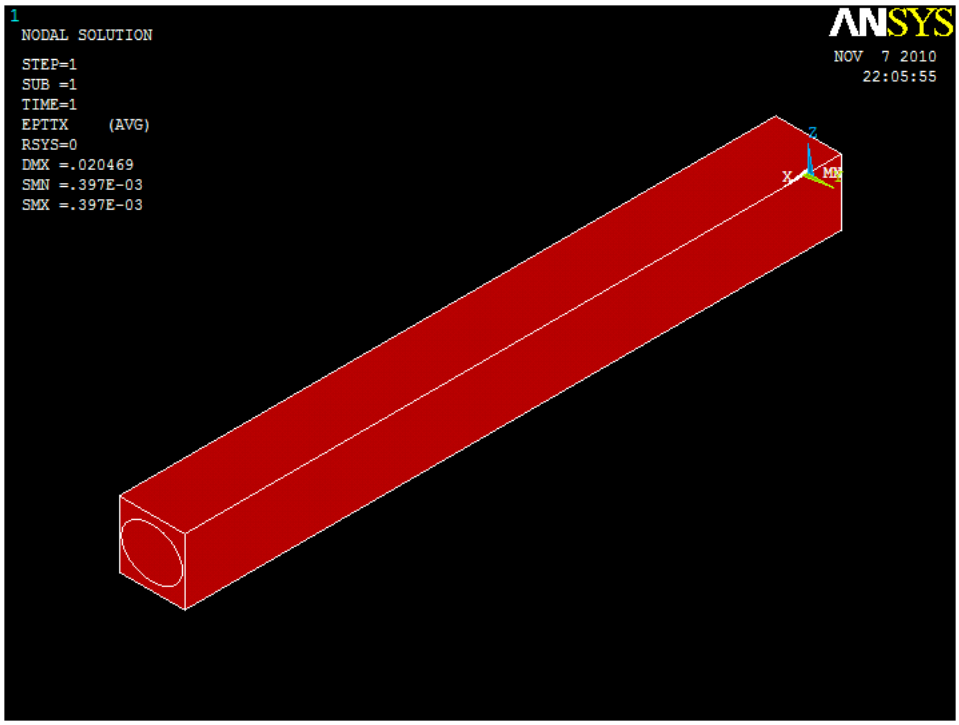

Figure 3.12. X-direction Total Strain in FEM Model with Elliptical Fiber.

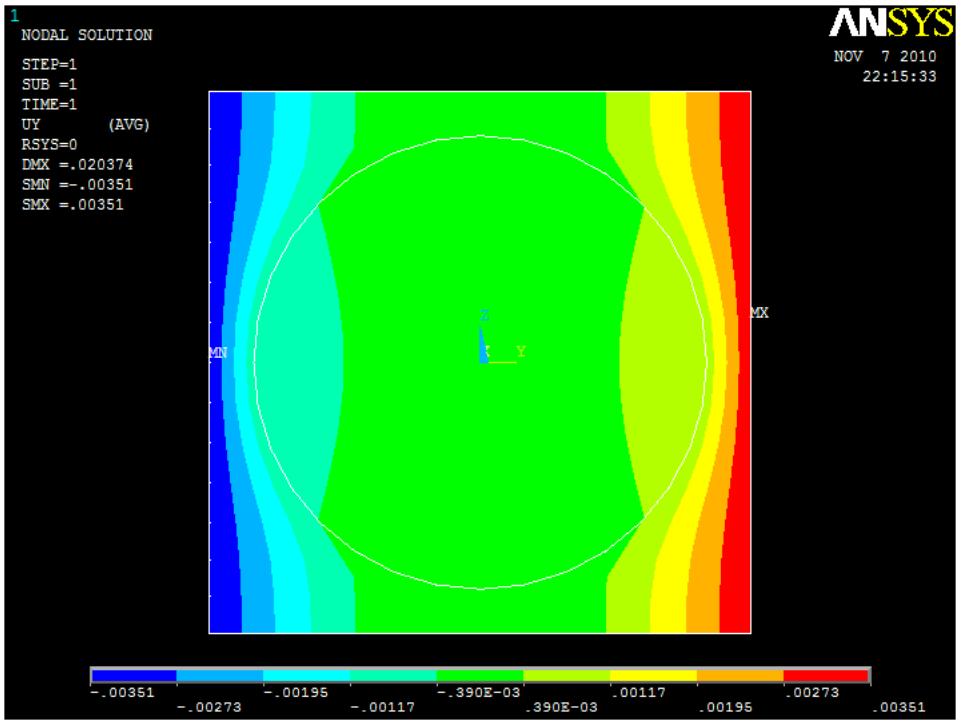

Figure 3.13. Y-Direction Deformation in FEM Model with Circular Fiber.

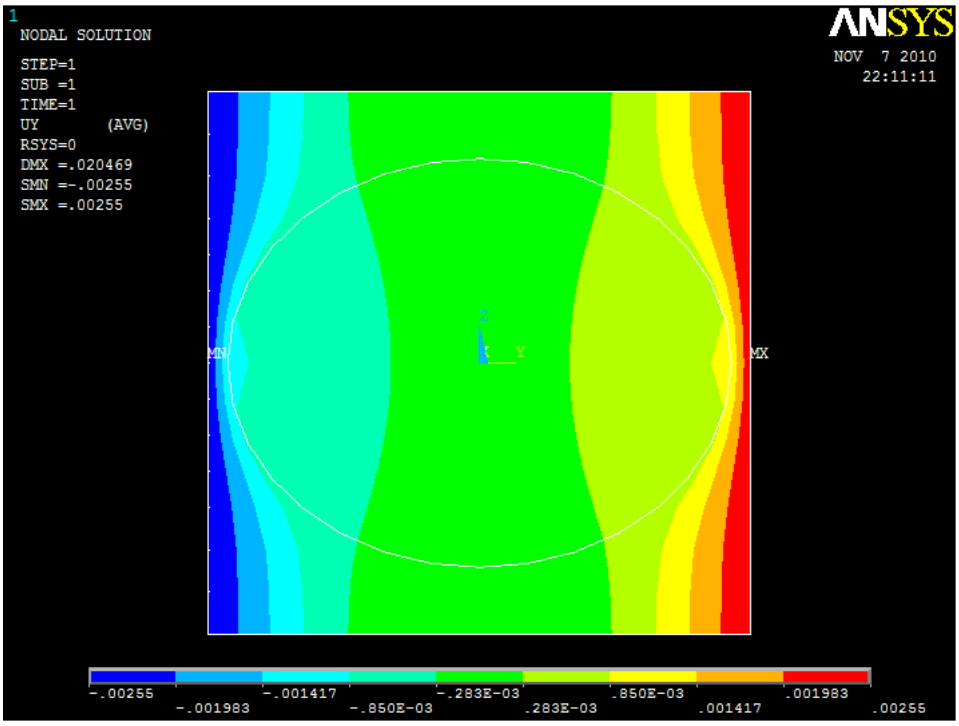

Figure 3.14. Y-Direction Deformation in FEM Model with Elliptical Fiber.

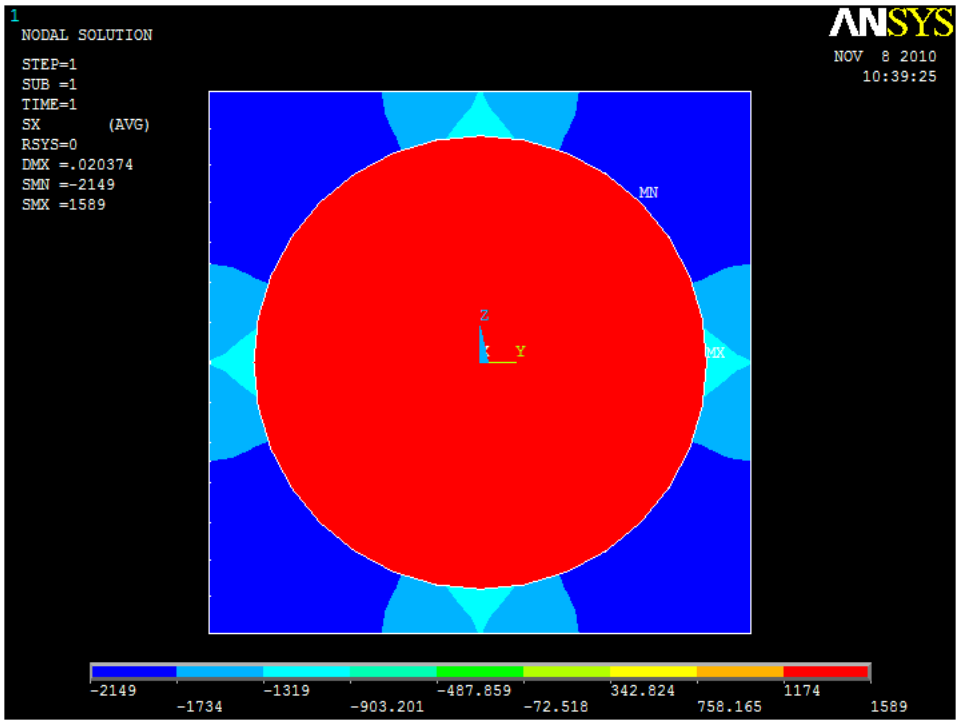

Figure 3.15. X-Direction Stress in FEM Model with Circular Fiber.

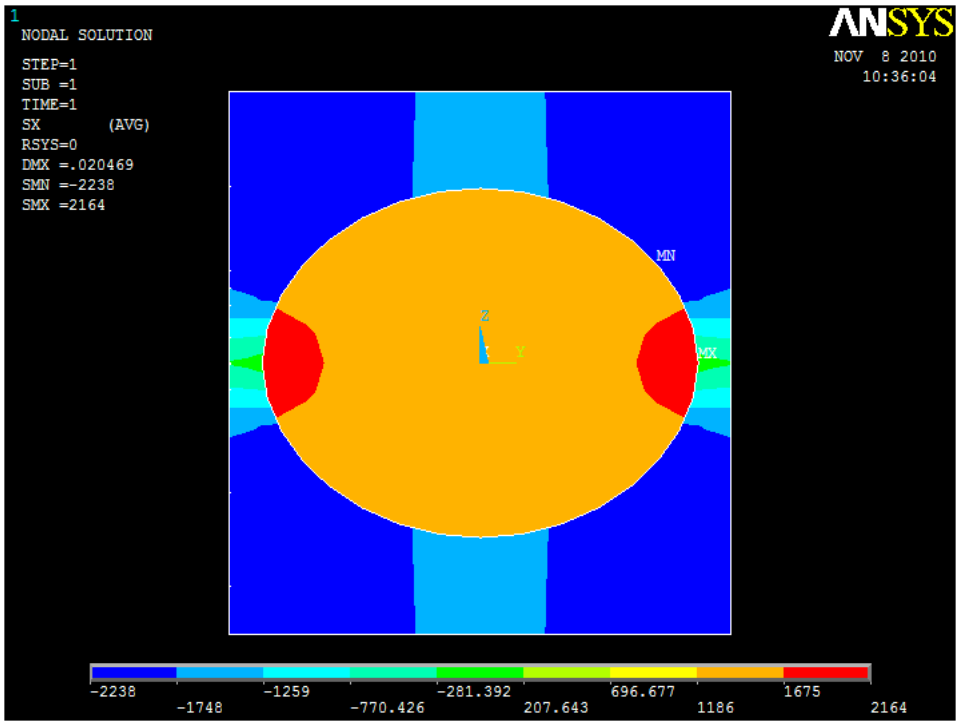

Figure 3.16. X-Direction Stress in FEM Model with Elliptical Fiber.

CHAPTER 4

NUMERICAL RESULTS AND DISCUSSIONS

A unit cell that contains a single E-glass fiber surrounded by the Epoxy 3501-6 matrix was used for this study. The material properties of fiber and matrix constituents are already shown in Chapter 3. The properties of y and z direction are assumed to be the transverse properties in the case of orthogonal fiber. The width and thickness of the unit cell are selected as 0.005 inch. In the fiber volume fraction (V_f) study, the fiber configuration is considered as the circular and then V_f is varied. On the other hand, V_f is fixed and the major and minor axis (a and b) are varied in the axial ratio study. The detail of all studies is described in the each section.

4.1 Effects of Fiber Volume Fraction on Effective Properties

In this section, the effects of the fiber volume fraction (V_f) on the effective moduli and Coefficients of Thermal Expansion (CTEs) are discussed. With this specified geometry of the model, V_f can be varied from 0 to 0.78. Figure 4.1 shows the size of circular fiber that is affected by increasing V_f. In both analytical solution and Rule of Mixture (ROM), the result can be accurately obtained by increasing 0.01 of V_f. However, the Finite Element Analysis (FEA) has to solve in each case of V_f. The number of analysis are 78 which is used too much time to proceed. Therefore, the 0.05 increase of V_f is used to reduce the time consuming.

Figures 4.2, 4.3, 4.4 and 4.5 separately display the variation of the effective moduli and CTEs with respect to V_f. In these figures, there are three different methods which are the analytical solution, ROM and FEA in each figure. The comparative

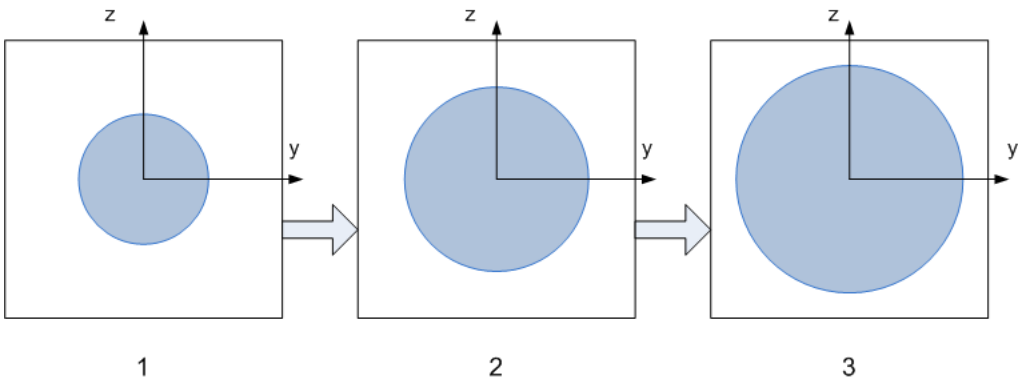

Figure 4.1. Fiber Size Varies with Fiber Volume Fraction.

data of these figures are also provided in Appendix D. Figures 4.2 and 4.3 show the comparison of E_1 and E_2 caculated by three different methods. Figures 4.4 and 4.5 show the same comparison of α_1 and α_2 as in the previous figures. As indicated in these figures, E_1 and α_1 agree very well among these three methods. The calculated values of E_2 and α_2 are different among all the methods. However, the present results of α_2 is closer to the finite element results. The difference of both transverse properties is depended increasingly on the fiber volume fraction. For the transverse properties, the difference between analytical solution and FEA reach a maximum about 16% at Vf=0.65. However, the difference between ROM and FEA is a maximum of 50% and 37% for E_2 and α_2, respectively. Therefore, the results between the analytical solution and FEA are closer than the ones between the ROM and FEA. In addition, there is a significant difference between in the presented and FEA results when the radius, r, is close to the width in E_2 variation because of the bad mesh in FEM.

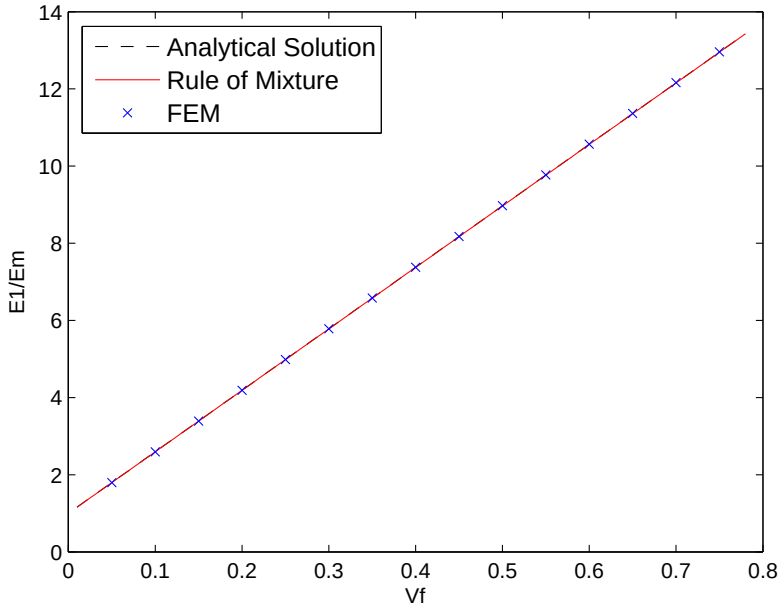

Figure 4.2. Longitudinal Modulus Respect with Fiber Volume Fraction.

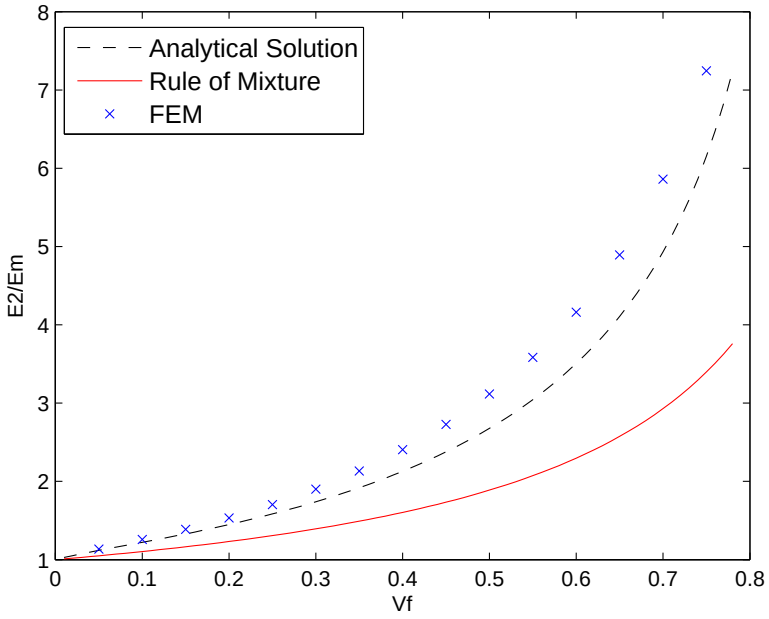

Figure 4.3. Transverse Modulus Respect with Fiber Volume Fraction.

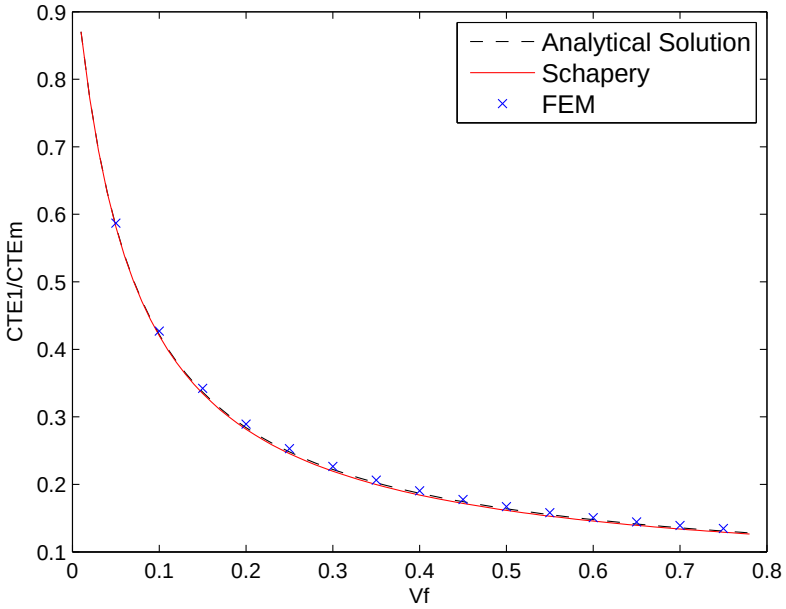

Figure 4.4. Longitudinal CTE Respect with Fiber Volume Fraction.

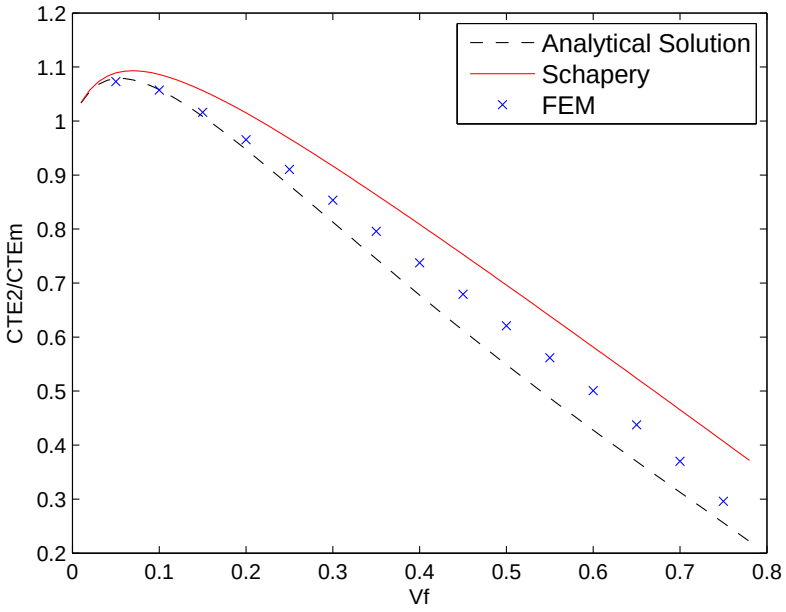

Figure 4.5. Transverse CTE Respect with Fiber Volume Fraction.

4.2 Effects of Fiber Configuration on the Effective Properties

The effects of fiber configuration on the effective moduli and CTEs are shown and discussed in this section, respectively. In the axial ratio (a/b) study, V_f is given as 0.55. Figure 4.6 illustrated the fiber configuration change with respect to the ratio of a/b. The detail of each approach is shown in Sec. 4.2.1 and 4.2.2.

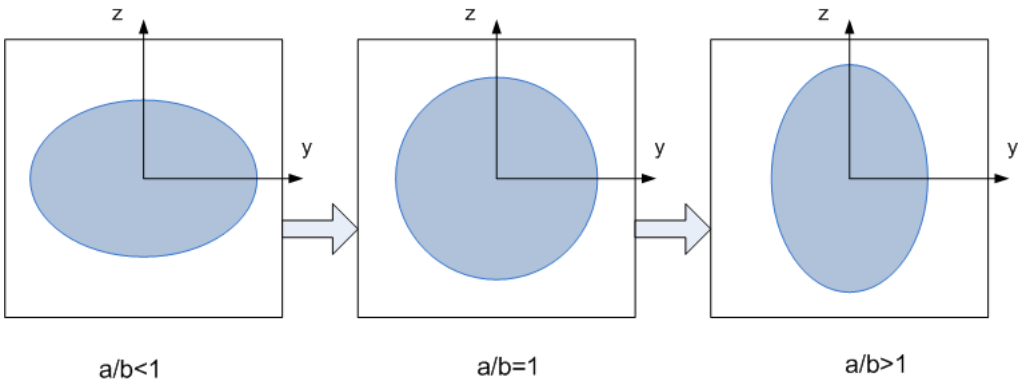

Figure 4.6. Fiber Shape Varies with Axial Ratio.

4.2.1 Effects of Fiber Configuration in Analytical Solution

The effects of fiber configurations on the stiffness were studied in the previous analytical solution by Wang and Chan[8]. Similarly, the effects of the fiber configurations on the effective moduli and CTEs are considered in this analytical solution. The radius, r, is firstly calculated from the fiber volume fraction and the width. The sizes of a and b are restricted by the width and thickness of the unit cell layer due to the specified fiber volume fraction. However, a and b can be obtained by assumed a and then calculate b from each a. For example, the major axis, a, is defined as 0.84 and gradually increased 0.01 until 1.19 in term of r and then the minor axis, b, can

be calculated for each value of a. For this example, the ratios of a/b are varying from 0.70 to 1.42.

The variations of the effective moduli and CTEs with respect to the a/b ratios for the analytical solution are presented in Figure 4.7 and 4.8. In addition, the comparative data are listed in appendix C. At the circular fiber, the results are normalized. When the a/b is increased, the fiber portion in z-direction is extended while the width of area does not change. The ratios of E_1 and α_1 slightly change in this results which agree with assumption that the longitudinal properties will not be significantly affected by the configuration of fiber. This is because the fiber volume fraction is fixed as the fiber configuration is changed. Unlikely, the E_2 is decreased as the axial ratio is increased. However, the transverse coefficient of thermal expansion, α_2, is increased for the increasing axial ratio. When the a/b is at the minimum and maximum, the cross sectional area of the unit cell fiber reinforced composite is more likely to the sanwich laminate. With the b is close to the width, the transverse properties will be gradually adjusted to be close to the longitudinal ones. ROM method is created to estimate the transverse properties of the sanwich composite. Therefore, the transverse properties is close to the ones from the ROM when the a is close to the width.

4.2.2 Effects of Fiber Configurations in Finite Element Analysis

Like the analytical solution, the finite element model is also designed in variation of the axial ratio. However, the finite element model is analyzed for each the axial ratio. Therefore, the numbers of the result in this study for FEA is less than for the analytical solution for reduce time consuming. The major axis, a, is gradually increased 0.02 of radius per the model for the finite element analysis. The example of

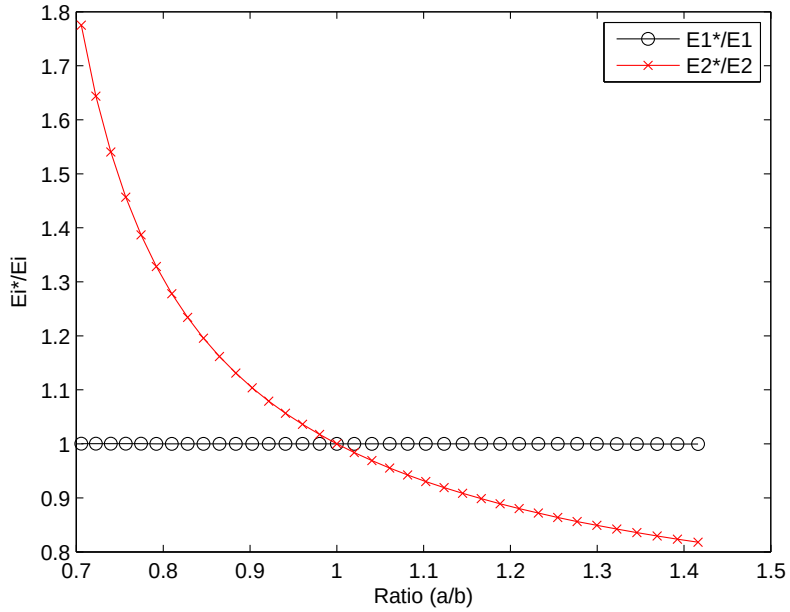

Figure 4.7. Moduli Ratio Respect with Axial Ratio in Analytical Solution.

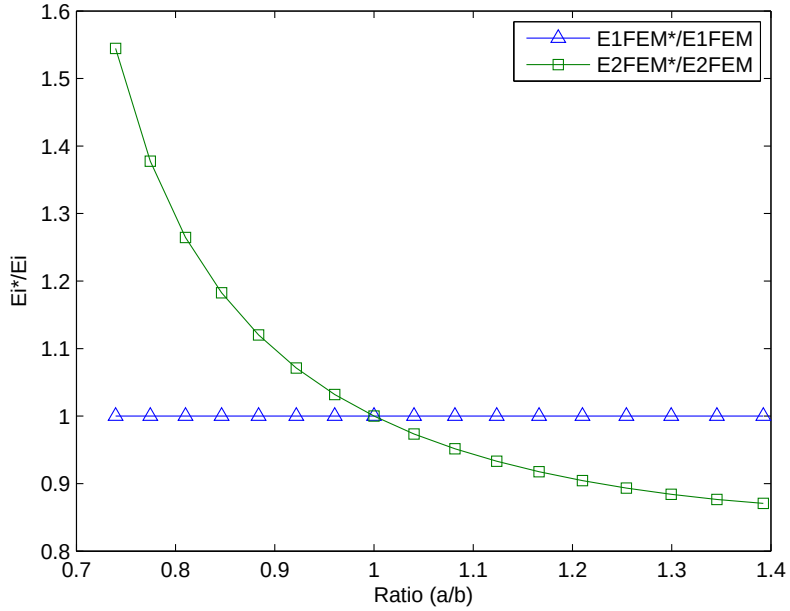

Figure 4.8. Moduli Ratio Respect with Axial Ratio in FEM.

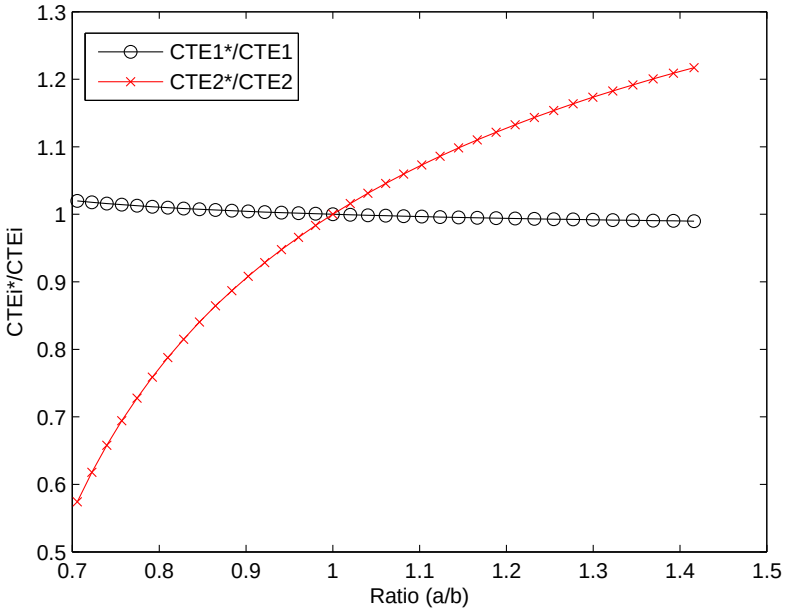

Figure 4.9. CTE Ratio Respect with Axial Ratio in Analytical Solution.

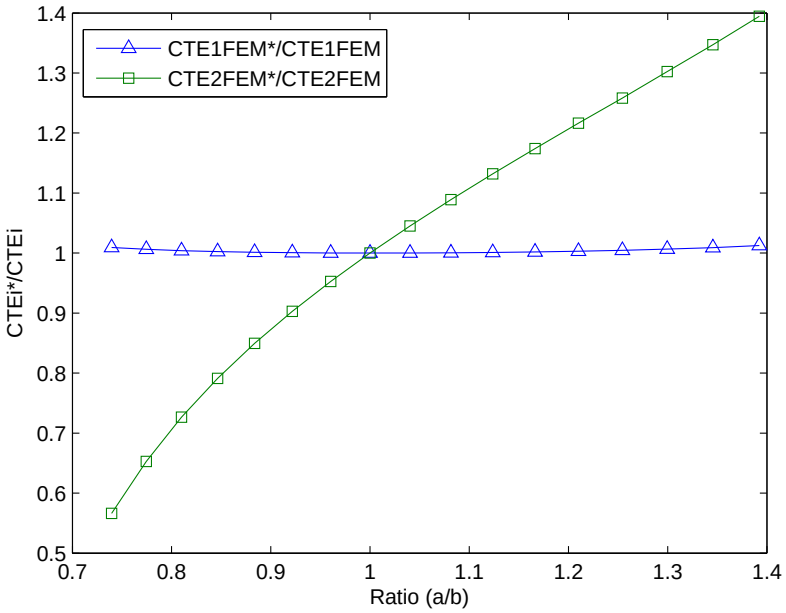

Figure 4.10. CTE Ratio Respect with Axial Ratio in FEM.

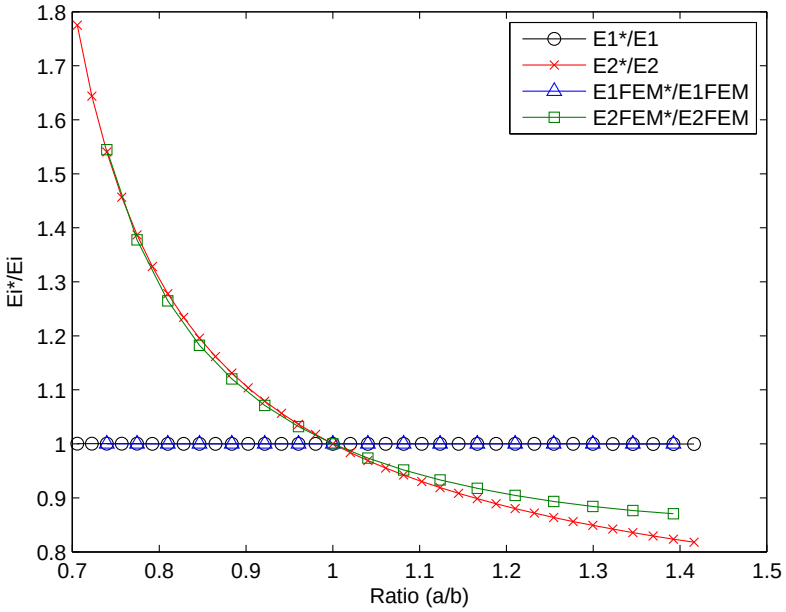

Figure 4.11. Moduli Ratio Respect with Axial Ratio in Both Solutions.

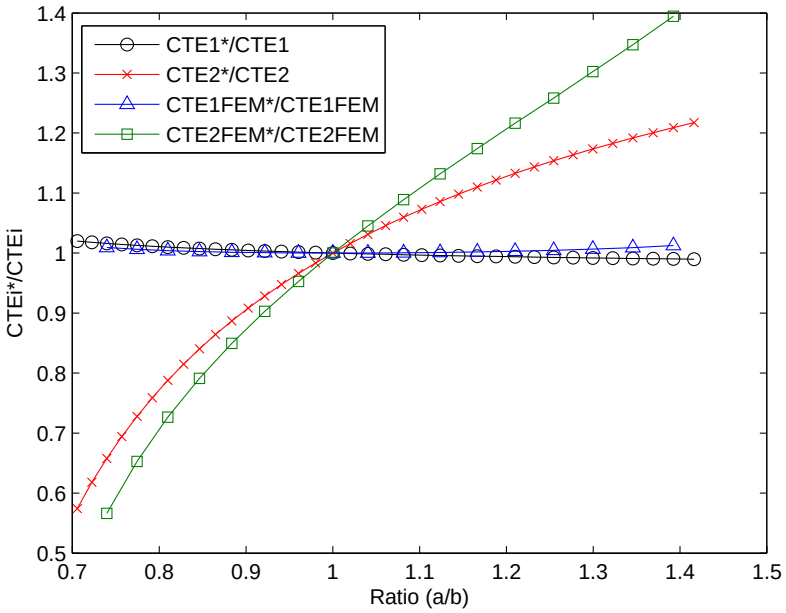

Figure 4.12. CTE Ratio Respect with Axial Ratio in Both Solutions.

the different model that change the a is already shown in Chapter 3, Figure 3.3 and 3.4.

The variations of the effective modul CTE with respect to the a/b ratios for the finite element analysis are shown in Figure 4.9 and 4.10. Similar to the variation from the analytical solution, the ratios of E_1 and α_1 is close to 1.00 (or 100%) as expect. For the ratios of E_2 and α_2 the curve is also similar to the one from analytical solution. However, the slopes of curves are greater. In addition, the E_2 result from FEA shows an error in the low axial ratio because the minor axis, b, is really close to the width.

Finally, the variations of the same property respect to the a/b from both analytical solution and FEA is also shown in the same figure for a comparison. Figure 4.11 and 4.12 are shown the variations of the effective moduli, E_1 and E_2, and the coefficients of thermal expansion, α_1 and α_2, respectively.

4.3 Stress Component Due to Thermal Expansion

Typically, the stress components can be evaluated at the specific nodes in FEM result. The certain position in x-y-z coordinate system of nodes is required to determine the stress components. However, the present method can also estimate the stress component in the specific z-position.

The stress components of the FEM result and present method in the various fiber configuration models are showed in Figure 4.13, 4.14 and 4.15. Figure 4.8 and 4.10 present the stress component in the elliptical fiber models while Figure 4.9 presents the result in the circular fiber model. Due to the difference of CTEs in fiber and matrix, the stress components are in both tension and compression. The fiber that is the lower CTE component is in tension while the matrix that is the higher CTE component is in compression.

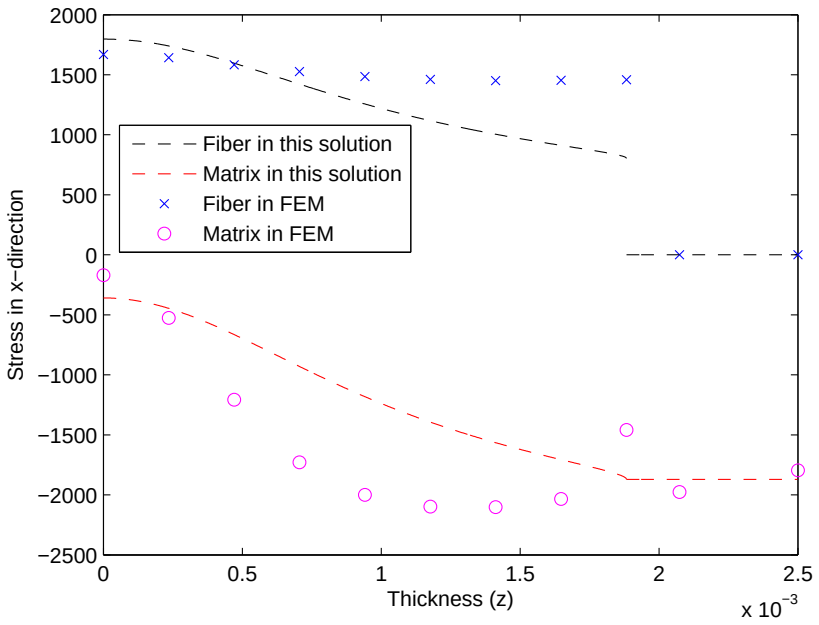

Figure 4.13. Stress Components for $a/b < 1$.

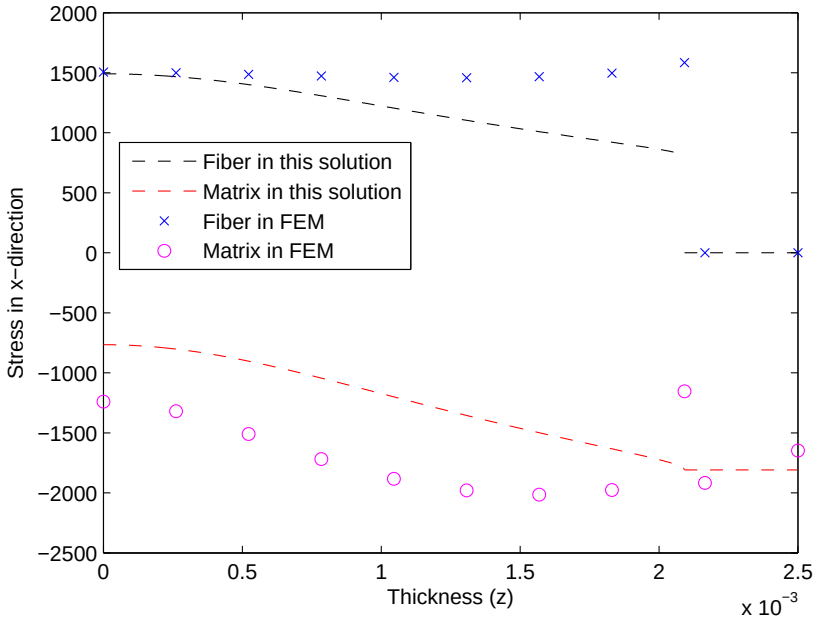

Figure 4.14. Stress Components for $a/b = 1$.

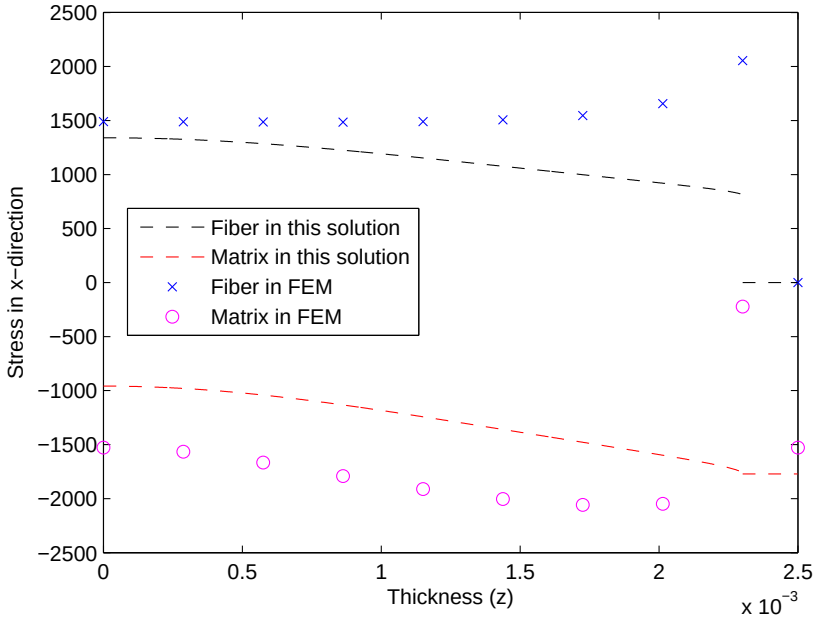

Figure 4.15. Stress Components for $a/b > 1$.

CHAPTER 5

CONCLUSION

A micromechanics model of a unit cell that contains a fiber and matrix was developed to evaluate the coefficients of thermal expansion (CTE) for fiber reinforced composite lamina. The model takes the fiber configuration into consideration in evaluation of the CTEs. Both circular and elliptical cross-sections of the fiber in the unit cell were considered in this study. The stress components of the fibers and the matrix in the unit cell under a temperature environment can also be obtained from the present model. An ANSY finite element model was used to validate the results of CTEs and the stress components of the fiber and the matrix in the unit cell obtained from the present method.

Effect of CTEs due to the fiber volume fraction (V_f) and the fiber configuration (a/b, semi-major axis to semi-minor axis ratio of elliptical cross-section) are studied. In V_f study, the results of the longitudinal CTE obtained by the present method are in excellent agreement with the results from finite element (FEA) and the Rule-of-Mixture (ROM) methods. However, the present results of the CTE along the transverse direction show a significant difference from the ROM results but close to the finite element results. The difference in the results is also dependent on the fiber volume fraction. In the fiber configuration study, the results of the longitudinal CTE for both elliptical and circular cross-sections of the fiber indicate no difference. However, the results in the transverse direction of CTE are significantly different from each other. It is found that the CTE along the transverse direction increases as the ratio of a/b increases.

It should be mentioned that the present model is applicable to the study of hygroscopic expansion coefficients since the similarity of the hygroscopic and thermal behavior.

APPENDIX A

THE INTEGRALS USED IN ANALYTICAL SOLUTIONS

The follow integrals are used for solving the analytical solution. The parameters p, p^*, q and q^* are used in the integrals also listed below.

$$p = Q_{22m} - Q_{22f} \tag{A.1}$$

$$q = Q_{22f} \tag{A.2}$$

$$p^* = Q_{66m} - Q_{66f} \tag{A.3}$$

$$q^* = Q_{66f} \tag{A.4}$$

For Composite Materials

The below list is presented the I_i parameters in composite materials.

$$I_1 = \int_{-a}^{a} V_f \, dz = \frac{ab\pi}{W} \tag{A.5}$$

$$I_2 = \int_{-a}^{a} {V_f}^2 \, dz = \frac{16ab^2\pi}{3W^2} \tag{A.6}$$

$$I_3 = \int_{-a}^{a} {V_f}^3 \, dz = \frac{3ab^3\pi}{W^3} \tag{A.7}$$

$$I_4 = \int_{-a}^{a} \frac{1}{pV_f + q} \, dz = \frac{aW}{2bp} \left\{ \pi - \frac{4}{\sqrt{1 - \left(\frac{2bp}{qW}\right)^2}} \arctan \sqrt{\frac{1 - \frac{2bp}{qW}}{1 + \frac{2bp}{qW}}} \right\} \tag{A.8}$$

$$I_4{}^* = \int_{-a}^{a} \frac{1}{p^*V_f + q^*}\, dz = \frac{aW}{2bp^*} \left\{ \pi - \frac{4}{\sqrt{1 - \left(\frac{2bp^*}{q^*W}\right)^2}} \arctan \sqrt{\frac{1 - \frac{2bp^*}{q^*W}}{1 + \frac{2bp^*}{q^*W}}} \right\} \tag{A.9}$$

$$I_5 = \int_{-a}^{a} \frac{V_f}{pV_f + q}\, dz = \frac{1}{p} \int_{-a}^{a} (1 - \frac{q}{pV_f + q})\, dz = \frac{2a}{p} - \frac{q}{p} I_4 \tag{A.10}$$

$$I_5{}^* = \int_{-a}^{a} \frac{V_f}{p^*V_f + q^*}\, dz = \frac{1}{p^*} \int_{-a}^{a} (1 - \frac{q^*}{p^*V_f + q^*})\, dz = \frac{2a}{p^*} - \frac{q^*}{p^*} I_4{}^* \tag{A.11}$$

$$I_6 = \int_{-a}^{a} \frac{{V_f}^2}{pV_f + q}\, dz = \frac{1}{p} \int_{-a}^{a} (V_f - \frac{qV_f}{pV_f + q})\, dz = \frac{I_1}{p} - \frac{q}{p} I_5 \tag{A.12}$$

$$I_6{}^* = \int_{-a}^{a} \frac{{V_f}^2}{p^*V_f + q^*}\, dz = \frac{1}{p^*} \int_{-a}^{a} (V_f - \frac{q^*V_f}{p^*V_f + q^*})\, dz = \frac{I_1}{p^*} - \frac{q^*}{p^*} I_5{}^* \tag{A.13}$$

$$I_7 = \int_{-a}^{a} \frac{{V_f}^3}{pV_f + q}\, dz = \frac{1}{p} \int_{-a}^{a} ({V_f}^2 - \frac{q{V_f}^2}{pV_f + q})\, dz = \frac{I_2}{p} - \frac{q}{p} I_6 \tag{A.14}$$

$$I_8 = \int_{-a}^{a} \frac{{V_f}^4}{pV_f + q}\, dz = \frac{1}{p} \int_{-a}^{a} ({V_f}^3 - \frac{q{V_f}^3}{pV_f + q})\, dz = \frac{I_3}{p} - \frac{q}{p} I_7 \tag{A.15}$$

$$I_9 = \int_{-a}^{a} zV_f\, dz = 0 \tag{A.16}$$

$$I_{10} = \int_{-a}^{a} \frac{z}{pV_f + q}\, dz = 0 \tag{A.17}$$

$$I_{10}{}^* = \int_{-a}^{a} \frac{z}{p^*V_f + q^*}\, dz = 0 \tag{A.18}$$

$$I_{11} = \int_{-a}^{a} \frac{zV_f}{pV_f + q}\, dz = 0 \tag{A.19}$$

$$I_{12} = \int_{-a}^{a} \frac{z{V_f}^2}{pV_f + q}\, dz = 0 \tag{A.20}$$

$$I_{13} = \int_{-a}^{a} z^2 V_f\, dz = \frac{a^3 b\pi}{W} \tag{A.21}$$

$$I_{14} = \int_{-a}^{a} \frac{z^2}{pV_f + q}\, dz = \int_{-a}^{a} \frac{a^2(1 - {V_f}^2)}{pV_f + q}\, dz = a^2(I_4 - I_6) \tag{A.22}$$

$${I_{14}}^* = \int_{-a}^{a} \frac{z^2}{p^*V_f + q^*}\, dz = \int_{-a}^{a} \frac{a^2(1 - {V_f}^2)}{p^*V_f + q^*}\, dz = a^2({I_4}^* - {I_6}^*) \tag{A.23}$$

$$I_{15} = \int_{-a}^{a} \frac{z^2 V_f}{pV_f + q}\, dz = \int_{-a}^{a} \frac{a^2(1 - {V_f}^2)V_f}{pV_f + q}\, dz = a^2(I_5 - I_7) \tag{A.24}$$

$$I_{16} = \int_{-a}^{a} \frac{z^2 {V_f}^2}{pV_f + q}\, dz = \int_{-a}^{a} \frac{a^2(1 - {V_f}^2){V_f}^2}{pV_f + q}\, dz = a^2(I_6 - I_8) \tag{A.25}$$

For Isotropic Materials

There is no different between $[Q]$ in the fiber and matrix. Hence, $p = 0$ and $p^* = 0$. Therefore, some parameters have to be revised.

The below list is presented the revised I parameters for the isotropic materials.

$$I_4 = \int_{-a}^{a} \frac{1}{pV_f + q}\, dz = \int_{-a}^{a} \frac{1}{q}\, dz = \frac{2a}{q} \tag{A.26}$$

$${I_4}^* = \int_{-a}^{a} \frac{1}{p^*V_f + q^*}\, dz = \int_{-a}^{a} \frac{1}{q^*}\, dz = \frac{2a}{q^*} \tag{A.27}$$

$$I_5 = \int_{-a}^{a} \frac{V_f}{pV_f + q}\, dz = \int_{-a}^{a} \frac{V_f}{q}\, dz = \frac{I_1}{q} \tag{A.28}$$

$$I_5{}^* = \int_{-a}^{a} \frac{V_f}{p^*V_f + q^*}\, dz = \int_{-a}^{a} \frac{V_f}{q^*}\, dz = \frac{I_1}{q^*} \tag{A.29}$$

$$I_6 = \int_{-a}^{a} \frac{{V_f}^2}{pV_f + q}\, dz = \int_{-a}^{a} \frac{{V_f}^2}{q}\, dz = \frac{I_2}{q} \tag{A.30}$$

$$I_6{}^* = \int_{-a}^{a} \frac{{V_f}^2}{p^*V_f + q^*}\, dz = \int_{-a}^{a} \frac{{V_f}^2}{q^*}\, dz = \frac{I_2}{q^*} \tag{A.31}$$

$$I_7 = \int_{-a}^{a} \frac{{V_f}^3}{pV_f + q}\, dz = \int_{-a}^{a} \frac{{V_f}^3}{q}\, dz = \frac{I_3}{q} \tag{A.32}$$

$$I_8 = \int_{-a}^{a} \frac{{V_f}^4}{pV_f + q}\, dz = \int_{-a}^{a} \frac{{V_f}^4}{q}\, dz = \frac{256ab^4}{15qW^4} \tag{A.33}$$

$$I_{14} = \int_{-a}^{a} \frac{z^2}{pV_f + q}\, dz = \int_{-a}^{a} \frac{a^2(1 - {V_f}^2)}{q}\, dz = \frac{a^2}{q}(2a - I_2) = a^2(I_4 - I_6) \tag{A.34}$$

$${I_{14}}^* = \int_{-a}^{a} \frac{z^2}{p^*V_f + q^*}\, dz = \int_{-a}^{a} \frac{a^2(1 - {V_f}^2)}{q^*}\, dz = \frac{a^2}{q^*}(2a - q^*) = a^2({I_4}^* - {I_6}^*) \tag{A.35}$$

$$I_{15} = \int_{-a}^{a} \frac{z^2 V_f}{pV_f + q}\, dz = \int_{-a}^{a} \frac{a^2(1 - {V_f}^2)V_f}{q}\, dz = \frac{a^2}{q}(I_1 - I_3) = a^2(I_5 - I_7) \tag{A.36}$$

$$I_{16} = \int_{-a}^{a} \frac{z^2 {V_f}^2}{pV_f + q}\, dz = \int_{-a}^{a} \frac{a^2(1 - {V_f}^2){V_f}^2}{q}\, dz = \frac{a^2}{q}(I_2 - qI_8) = a^2(I_6 - I_8) \tag{A.37}$$

APPENDIX B

FEM CODES FOR ANSYS 11.0 PROGRAMS

B.1 ANSYS 11.0 Program for Thermal Expansion Case in Quarter Model

```
!!!!!!!!!!!!!!!!!!!!!!!!!!!!!!!!!!!!!!!!!!!!!!!!!!!!!!!!!!!!!!!!!!!!!!!!!!!!!!!!!!!!!!!!!!!!!!!!!!!!!!!!!!!
/UNITS,BIN
/PREP7
!
! Define Parameter (in)
!
W=5
Pi=3.141592653589793
Vf=0.55
R=(sqrt(Vr/Pi))*W
a=1.00*R
b=Vf*W*W/(Pi*a)
L=10*W
!
! Define Keypoints
!
K,1,0,0,0
K,2,0,R/2,0
K,3,0,R,0
K,4,0,W/2,0
K,5,0,R/2,R/2
K,6,0,R/(sqrt(2)),R/(sqrt(2))
K,7,0,W/2,W/2
K,8,0,0,R/2
K,9,0,0,R
```

```
K,10,0,0,W/2
K,11,0, b/(sqrt(2)),W/2
K,12,0,W/2, a/(sqrt(2))
!
! Define Lines and Area !
L,1,2
L,2,3
L,5,6
L,1,8
L,8,9
L,2,5
L,5,8
L,4,12
L,12,7
L,7,11
L,11,10
LARC,3,6,1,R
LARC,6,9,1,R
FLST,2,4,4
FITEM,2,2
FITEM,2,12
FITEM,2,6
FITEM,2,3
AL,P51X
FLST,2,4,4
FITEM,2,3
```

FITEM,2,13

FITEM,2,7

FITEM,2,5

AL,P51X

FLST,2,4,4

FITEM,2,6

FITEM,2,1

FITEM,2,4

FITEM,2,7

AL,P51X

FLST,2,3,5,ORDE,2

FITEM,2,1

FITEM,2,-3

ARSCALE,P51X, , ,1,b/R,a/R, ,1,1

L,6,11

L,6,12

L,3,4

L,9,10

FLST,2,4,4

FITEM,2,8

FITEM,2,16

FITEM,2,12

FITEM,2,15

AL,P51X

FLST,2,4,4

FITEM,2,9

```
FITEM,2,15
FITEM,2,10
FITEM,2,14
AL,P51X
FLST,2,4,4
FITEM,2,11
FITEM,2,14
FITEM,2,13
FITEM,2,17
AL,P51X
!
! Element Definition
!
ET,1,SHELL93
ET,2,SOLID95
! material property number 1 E-glass
MP,EX,1,10.5e6
MP,EY,1,10.5e6
MP,EZ,1,10.5e6
MP,PRXY,1,0.23
MP,PRYZ,1,0.23
MP,PRXZ,1,0.23
MP,GXY,1,4.3e6
MP,GYZ,1,4.3e6
MP,GXZ,1,4.3e6
MP,CTEX,1,2.8e-6
```

```
MP,CTEY,1,2.8e-6
MP,CTEZ,1,2.8e-6
! material property number 2 Epoxy 3501-6
MP,EX,2,0.62e6
MP,EY,2,0.62e6
MP,EZ,2,0.62e6
MP,PRXY,2,0.35
MP,PRYZ,2,0.35
MP,PRXZ,2,0.35
MP,GXY,2,0.24e6
MP,GYZ,2,0.24e6
MP,GXZ,2,0.24e6
MP,CTEX,2,25e-6
MP,CTEY,2,25e-6
MP,CTEZ,2,25e-6
/VIEW,1,1,1,1
/ANG,1
/REP,FAST
APLOT
!
! Meshing 2-D
!
AESIZE,ALL,W/10
FLST,5,3,5,ORDE,2
FITEM,5,1
FITEM,5,-3
```

```
CM,_Y,AREA
ASEL, , , ,P51X
CM,_Y1,AREA
CMSEL,S,_Y
!*
CMSEL,S,_Y1
AATT, 1, , 1, 0,
CMSEL,S,_Y
CMDELE,_Y
CMDELE,_Y1
!*
MSHAPE,0,2D
MSHKEY,1
!*
FLST,5,3,5,ORDE,2
FITEM,5,1
FITEM,5,-3
CM,_Y,AREA
ASEL, , , ,P51X
CM,_Y1,AREA
CHKMSH,'AREA'
CMSEL,S,_Y
!*
AMESH,_Y1
!*
CMDELE,_Y
```

```
CMDELE,_Y1
CMDELE,_Y2
!*
FLST,5,3,5,ORDE,2
FITEM,5,4
FITEM,5,-6
CM,_Y,AREA
ASEL, , , ,P51X
CM,_Y1,AREA
CMSEL,S,_Y
!*
CMSEL,S,_Y1
AATT, 2, , 1, 0,
CMSEL,S,_Y
CMDELE,_Y
CMDELE,_Y1
!*
FLST,5,3,5,ORDE,2
FITEM,5,4
FITEM,5,-6
CM,_Y,AREA
ASEL, , , ,P51X
CM,_Y1,AREA
CHKMSH,'AREA'
CMSEL,S,_Y
!*
```

```
AMESH,_Y1
!*
CMDELE,_Y
CMDELE,_Y1
CMDELE,_Y2
!*
/UI,MESH,OFF
!
! 3D Mesh Generation by Extruding
!
TYPE, 2
EXTOPT,ESIZE,80,0,
EXTOPT,ACLEAR,0
!*
EXTOPT,ATTR,0,0,0
MAT,1
REAL,_Z4
ESYS,0
!*
FLST,2,3,5,ORDE,2
FITEM,2,1
FITEM,2,-3
VEXT,P51X, , ,L,0,0,,,,
TYPE, 2
EXTOPT,ESIZE,80,0,
EXTOPT,ACLEAR,0
```

```
!*
EXTOPT,ATTR,0,0,0
MAT,2
REAL,_Z4
ESYS,0
!*
FLST,2,3,5,ORDE,2
FITEM,2,4
FITEM,2,-6
VEXT,P51X, , ,L,0,0,,,,
!
!* Deleting 2D Mesh
!
FLST,2,92,5,ORDE,2
FITEM,2,1
FITEM,2,-92
ACLEAR,P51X
NUMMRG,NODE
!
! Boundary Conditions
!
! Ux = 0 @ x = 0
NSEL,S,LOC,X,0,
D,ALL,UX,0
ALLSEL
! Uy = 0 @ y = 0
```

NSEL,S,LOC,Y,0,

D,ALL,UY,0,

ALLSEL

! Uz = 0 @ z = 0

NSEL,S,LOC,Z,0,

D,ALL,UZ,0,

ALLSEL

! Coupling in X-direction @ X=L, in Y-direction @ Y=W/2 and in Z-direction @ Z=W/2

NSEL,S,LOC,X,L,

CP,3,UX,ALL

NSEL,S,LOC,Y,W/2,

CP,4,UY,ALL

NSEL,S,LOC,Z,W/2,

CP,5,UZ,ALL

ALLSEL

!

! Load Conditions

!

! Tref = 70 and T = 170. Therefore, ΔT = 100

ANTYPE,0

TREF,70,

BFUNIF,TEMP,170

B.2 ANSYS 11.0 Program for Longitudianl Load Case in Quarter Model (Only Load Conditions)

```
! Load Conditions
!

NSEL,S,LOC,X,L,
NSEL,R,LOC,Y,0,
NSEL,R,LOC,Z,0,
F,all,Fx,1
ALLSEL
```

B.3 ANSYS 11.0 Program for Transverse Load Case in Quarter Model (Only Load Conditions)

```
! Load Conditions
!

NSEL,S,LOC,X,0,
NSEL,R,LOC,Y,W/2,
NSEL,R,LOC,Z,0,
F,all,FY,1
ALLSEL
```

APPENDIX C

THE COMPARATIVE DATA

Table C.1. Comparison of the Longitudinal Modulus Respect with the Fiber Volume Fraction

Fiber Volume Fraction	The Longitudinal Modulus, E_1/E_m from		
	Analytical Solution	Rule of Mixture	FE Analysis
0.05	1.7969	1.7968	1.7971
0.10	2.5940	2.5935	2.5953
0.15	3.3910	3.3903	3.3928
0.20	4.1881	4.1871	4.1901
0.25	4.9852	4.9839	4.9875
0.30	5.7822	5.7806	5.7846
0.35	6.5792	6.5774	6.5818
0.40	7.3761	7.3742	7.3788
0.45	8.1730	8.1710	8.1757
0.50	8.9699	8.9677	8.9727
0.55	9.7667	9.7645	9.7696
0.60	10.5635	10.5613	10.5665
0.65	11.3603	11.3581	11.3635
0.70	12.1571	12.1548	12.1608
0.75	12.9538	12.9516	12.9589

Table C.2. Comparison of the Transverse Modulus Respect with the Fiber Volume Fraction

Fiber Volume Fraction	The Transverse Modulus, E_2/E_m from		
	Analytical Solution	Rule of Mixture	FE Analysis
0.05	1.1182	1.0494	1.1362
0.10	1.2212	1.1039	1.2576
0.15	1.3291	1.1643	1.3873
0.20	1.4486	1.2318	1.5338
0.25	1.5839	1.3076	1.7029
0.30	1.7390	1.3933	1.9001
0.35	1.9186	1.4911	2.1316
0.40	2.1288	1.6035	2.4046
0.45	2.3777	1.7344	2.7286
0.50	2.6771	1.8885	3.1158
0.55	3.0442	2.0726	3.5845
0.60	3.5060	2.2966	4.1618
0.65	4.1078	2.5748	4.8932
0.70	4.9326	2.9297	5.8620
0.75	6.1546	3.3981	7.2454

Table C.3. Comparison of the Longitudinal CTE Respect with the Fiber Volume Fraction

Fiber Volume Fraction	The Longitudinal CTE, α_1/α_m from		
	Analytical Solution	Schapery's Method	FE Analysis
0.05	0.5824	0.5815	0.5870
0.10	0.4217	0.4201	0.4271
0.15	0.3367	0.3346	0.3421
0.20	0.2840	0.2817	0.2892
0.25	0.2482	0.2456	0.2529
0.30	0.2222	0.2195	0.2265
0.35	0.2024	0.1998	0.2064
0.40	0.1868	0.1843	0.1905
0.45	0.1743	0.1718	0.1776
0.50	0.1639	0.1615	0.1670
0.55	0.1552	0.1529	0.1581
0.60	0.1478	0.1456	0.1506
0.65	0.1413	0.1394	0.1443
0.70	0.1358	0.1339	0.1390
0.75	0.1308	0.1291	0.1347

Table C.4. Comparison of the Transverse CTE Respect with the Fiber Volume Fraction

Fiber Volume Fraction	The Transverse CTE, α_2/α_m from		
	Analytical Solution	Schapery's Method	FE Analysis
0.05	1.0785	1.0891	1.0731
0.10	1.0583	1.0862	1.0571
0.15	1.0087	1.0564	1.0161
0.20	0.9473	1.0150	0.9655
0.25	0.8809	0.9675	0.9104
0.30	0.8128	0.9166	0.8535
0.35	0.7447	0.8634	0.7957
0.40	0.6777	0.8087	0.7376
0.45	0.6123	0.7529	0.6794
0.50	0.5489	0.6963	0.6209
0.55	0.4873	0.6392	0.5616
0.60	0.4277	0.5816	0.5009
0.65	0.3696	0.5236	0.4377
0.70	0.3127	0.4653	0.3702
0.75	0.2561	0.4068	0.2958

Table C.5. Comparisons of the Effective Moduli and CTE of Elliptical Fiber and Circular Fiber with Respect to The Axial Ratio in Finite Element Analysis

Axial Ratio	E_1^*/E_1	E_2^*/E_2	α_1^*/α_1	α_2^*/α_2
0.7396	100.02%	154.45%	100.94%	56.61%
0.7744	100.01%	137.76%	100.62%	65.29%
0.8100	100.00%	126.46%	100.39%	72.65%
0.8464	100.00%	118.25%	100.24%	79.12%
0.8836	100.00%	112.01%	100.12%	84.94%
0.9216	100.00%	107.12%	100.05%	90.29%
0.9604	100.00%	103.20%	100.01%	95.28%
1.0000	100.00%	100.00%	100.00%	100.00%
1.0404	100.00%	97.36%	100.01%	104.52%
1.0816	100.00%	95.16%	100.05%	108.90%
1.1236	100.00%	93.31%	100.11%	113.18%
1.1664	100.00%	91.76%	100.20%	117.41%
1.2100	100.00%	90.45%	100.31%	121.64%
1.2544	100.01%	89.34%	100.46%	125.83%
1.2996	100.01%	88.41%	100.66%	130.24%
1.3456	100.02%	87.64%	100.90%	134.71%
1.3924	100.02%	87.08%	101.24%	139.44%

Table C.6. Comparisons of the Effective Moduli and CTE of Elliptical Fiber and Circular Fiber with Respect to The Axial Ratio in Analytical Solution

Axial Ratio	E_1^*/E_1	E_2^*/E_2	α_1^*/α_1	α_2^*/α_2
0.7396	100.02%	154.04%	101.60%	65.78%
0.7744	100.02%	138.70%	101.27%	72.78%
0.8100	100.02%	127.79%	100.99%	78.79%
0.8464	100.01%	119.56%	100.75%	84.04%
0.8836	100.01%	113.12%	100.53%	88.69%
0.9216	100.01%	107.91%	100.33%	92.85%
0.9604	100.00%	103.61%	100.16%	96.60%
1.0000	100.00%	100.00%	100.00%	100.00%
1.0404	100.00%	96.91%	99.85%	103.11%
1.0816	100.00%	94.24%	99.72%	105.96%
1.1236	99.99%	91.91%	99.60%	108.59%
1.1664	99.99%	89.85%	99.48%	111.02%
1.2100	99.99%	88.02%	99.38%	113.27%
1.2544	99.99%	86.38%	99.28%	115.37%
1.2996	99.99%	84.91%	99.19%	117.34%
1.3456	99.99%	83.57%	99.10%	119.17%
1.3924	99.98%	82.36%	99.02%	120.90%

REFERENCES

[1] R. Kulkarni and O. Ochoa, "Transverse and longitudinal cte measurements of carbon fibers and their impact on interfacial residual stresses in composite," *Journal of Composite Materials*, vol. 40, 8.

[2] H. G. Kia, "Thermal expansion of sheet molding compound materials," *Journal of Composite Materials*, vol. 42(7), pp. 681–695, 2008.

[3] R. A. Schapery, "Thermal expansion coefficient of composite materials based on energy principles," *Journal of Composite Materials*, vol. 2(3), pp. 380–404, 1968.

[4] B. W. Rosen and Z. Hashin, "Effective thermal expansion coefficients and specific heats of composite materials," *International Journal of Engineering Science*, vol. 8, pp. 157–173, 1970.

[5] G. P. Tandon and A. Chatterjee, "The transverse coefficient of thermal expansion of a unidirection composite," *Journal of Material Science*, vol. 26, pp. 2759–2764, 1991.

[6] T. Ishikawa, K. Koyama, and S. Kobayashi, "Thermal expansion coefficients of unidirectional composites," *Journal of Composite Materials*, vol. 12, pp. 153–168, 1978.

[7] J. D. D. Melo and D. W. Radford, "Determination of the elastic constants of a transversely isotropic lamina using laminate coefficients of thermal expansion," *Journal of Composite Materials*, vol. 36(11), pp. 1321–1329, 2002.

[8] J. S. Wang and W. S. Chan, "Effects of defects on the buckling load of rodpack laminates," *Journal of American Helicopter Society*, vol. 45, pp. 216–221, 2000.

[9] W. Yu and T. Tang, "A variational asymptotic micromechanics model for predicting thermoelastic properties of heterogeneous materials," *International Journal of Solids and Structures*, vol. 44, pp. 7510–7525, 2007.

[10] M. R. Islam, S. G. Sjolind, and A. Pramila, "Finite element analysis of linear thermal expansion coefficients of unidirectional cracked composite," *Journal of Composite Materials*.

[11] Z. H. Karadeniz and D. Kumlutas, "A numerical study on the coefficients of thermal expansion of fiber reinforced composite materials," *Composite Structures*, vol. 78, pp. 1–10, 2007.

[12] I. M. Daniel and O. Ishai, *Engineering Mechanics of Composite Materials*. New York: Oxford University Press, 2006.

BIOGRAPHICAL STATEMENT

Nittapon Srisuk was born in Nakhon Nayok, Thailand, in August 1983. He received his B.S. degree in Aeronautical Engineering from Royal Thai Air force Academy, Thailand, in 2005. From 2005 to 2008, he was in the Air Technical Division, Directorate of Aeronautical Engineering as an engineer. In 2008, he pursued his master degree in Aerospace Engineering at The University of Texas at Arlington.